Journal of
ENERGY TECHNOLOGY

Journal of
ENERGY TECHNOLOGY

VOLUME 11 / Issue 1

JOURNAL OF ENERGY TECHNOLOGY

Spoštovani bralci revije Journal of energy technology (JET)

Potrebe po toplotni energiji globalno gledano presegajo več kot polovico vseh potreb po energiji. Trenutno pridobivamo večino toplotne energije iz ogljikovodikov in njihovih derivatov, nekaj malega tudi s pomočjo obnovljivih virov energije. Pričakujemo, da bo prav proizvodnja toplotne energije iz obnovljivih virov v prihodnje bistveno presegla sedanje vrednosti. V ta namen bi lahko uporabili vse vrste obnovljivih virov energije. Še posebej zanimiva je izraba sončne energije s sončnimi kolektorji s preko 60 % izkoristka. Poznamo več sistemov pridobivanja toplotne energije s soncem: s ploščnimi kolektorji, vakuumski kolektorji, toplozračnimi kolektorji in kolektorji, kjer lahko istočasno pridobivamo sončno in toplotno energijo. Vse pogosteje se uporabljajo tudi sončni paneli, s katerimi obložimo npr. fasade hiš in na ta način pridobimo dobršen del energije za potrebe ogrevanja hiš in industrijskih objektov. Na tem področju veliko energije v razvoj namenjajo tudi slovenska podjetja.

Jurij AVSEC
odgovorni urednik revije JET

Dear Readers of the Journal of Energy Technology (JET)

The demand for thermal energy accounts for more than half of all the world's total energy needs. We currently generate most of that heat from hydrocarbons and their derivatives. Some small amounts are produced through renewable energy sources throughout the world. In the future, it is expected that the production of heat from renewable sources will significantly exceed the current level. For this purpose, all types of renewable energy sources could be used. Particularly interesting is the use of solar energy with solar collectors, which have a yield of over 60%. Currently, there are several solar thermal generation systems, such as plate collectors, vacuum collectors, hot-air collectors and collectors, with which solar and thermal energy can be simultaneously obtained. In the foreground, there are also solar panels, which can be used to cover the facades of houses. In this way, they could acquire a good portion of the energy required for home and industrial heating. Slovenian companies are highly active in development in this field.

Jurij AVSEC
Editor-in-chief of JET

Table of Contents / Kazalo

PERFORMANCE ANALYSIS OF PHOTOVOLTAIC SYSTEMS IN THE BRESTANICA THERMAL POWER PLANT

ANALIZA UČINKOVITOSTI SONČNIH ELEKTRARN V TE BRESTANICA

Bojan Vovčko[R]

Keywords: performance ratio, energy yield, photovoltaic system, solar cell, temperature coefficient of efficiency, solar irradiation, inclination angle, azimuth angle, partial shading

Abstract

This paper deals with the performance ratio and energy yield of three photovoltaic systems (MFE TEB 1-3) in the Brestanica thermal power plant (TE Brestanica). The objective of this paper is to analyse these two parameters according to the different types of solar cells (amorphous/monocrystalline silicon), non-ideal inclination, and azimuth angles of PV modules in different seasons. The analysis was made on the basis of operating data of MFE TEB 1-3 for the period from 2011 to 2016. Performance ratio is one of the most important parameters in the assessment of the quality of photovoltaic systems; it represents the ratio between the actual energy produced and the theoretical energy produced by a photovoltaic system and shows the proportion of energy that is available for transmission to the electricity network after deducting lost energy. In contrast, the energy yield represents the ratio between the actual energy produced and the nominal power of the photovoltaic system. The results show a significant influence of temperature coefficient, as well as the inclination and azimuth angles of the PV modules on the performance ratio and the energy yield.

[R] Corresponding author: Bojan Vovčko, B.Sc.(E.E.), TE Brestanica d.o.o., Cesta prvih borcev 18, E-mail address: bojan.vovcko@teb.si

Povzetek

Prispevek obravnava faktor učinkovitosti in energijski izplen treh sončnih elektrarn (MFE TEB 1-3), katere ima v lasti Termoelektrarna Brestanica. Cilj tega prispevka je narediti analizo teh dveh parametrov glede na različno vrsto sončnih celic (amorfni/monokristalni silicij), neidealnim naklonskim in azimutnim kotom sončnih modulov v različnih letnih časih. Analiza je bila narejena na osnovi obratovalnih podatkov za obdobje od 2011 do 2016. Faktor učinkovitosti je eden izmed najpomembnejših parametrov pri ocenjevanju kakovosti sončnih elektrarn in predstavlja razmerje med dejansko in predvideno proizvodnjo električne energije sončne elektrarne ter prikazuje delež energije, ki je na voljo za prenos v omrežje po odbitku izgubljene energije, energijski izplen pa predstavlja razmerje med dejansko proizvedeno električno energijo in nazivno močjo sončne elektrarne. Rezultati kažejo precejšen vpliv temperaturnega koeficienta, naklonskega in azimutnega kota sončnih modulov na faktor učinkovitosti in energijski izplen.

1   INTRODUCTION

In TE Brestanica, we are very much aware of the importance of environmentally friendly energy production, so we started to direct our activities to renewable energy sources (RES) almost a decade ago. We have actively participated in the construction, operation, and maintenance of hydroelectric power plants at the lower Sava River. From the start of this project in 2002, and in 2008, we also started with activities on the development and construction of photovoltaic systems. In February 2009, we had a trial run of the first photovoltaic system (MFE TEB 1), with a rated output of 38 kW$_p$. At the end of March 2010, we had a trial run of another two photovoltaic systems: MFE TEB 2 integrated in the roof of a covered parking lot with a rated output of 82 kW$_p$ and MFE TEB 3 with nominal power 50 kW$_p$, which is placed on the roof of gas turbine (GT) units PB4 and PB5. The total installed power of photovoltaic systems in TEB is 170 kW$_p$.

For the MFE TEB 2, integrated into the parking lot's roof, we obtained the status of an integrated photovoltaic system (higher feed-in tariff) from the Energy Agency in 2010. Additionally, in 2011, we received a "Bronze Award for the Best Innovations in 2010" for the covered parking lot from the Posavje Regional Chamber of Commerce and Industry of Slovenia (CCIS).

In the case of our photovoltaic system projects, we mainly pursued the vision of placement of photovoltaic systems on the TE Brestanica location in the most architecturally acceptable and useful way. Furthermore, in the design phase of photovoltaic systems, we were quite experimental, which means that we tried to use as many different materials and implementation methods as possible so that would will be able to determine the advantages and disadvantages.

Several researchers, *[1]–[7]*, have analysed the performance ratio of integrated photovoltaic system. In this paper, we will focus on the analysis of the performance ratio (*PR*) and the energy yield (*Y*), in order to verify the performance and quality of the photovoltaic system in TE Brestanica, depending on the type of solar cells, inclination and azimuth angles, partial shading, weather conditions and on the duration of the operation. The analysis will be done on the basis of operating data for a six-year period from 2011 to 2016.

2.1   Photovoltaic system MFE TEB 1

The first photovoltaic system in TE Brestanica, MFE TEB 1, was built as a part of the energy efficient renovation of the business building, which included the implementation of an energy efficient facade and the replacement of the asbestos roof covering. We started with renovation of the business facility in November 2008 and completed it in spring 2009. As a new roof covering, we used the Trimo SNV-3L sandwich panels with integrated thin-film PV modules Unisolar PVL 136 from amorphous silicon. The market name of the panel with a PV module, shown in Figure 1, is Trimo EcoSolar PV.

The key reasons for using thin-film PV modules from amorphous silicon are:

- Low temperature coefficient of the PV module output power (-0.21%/°C): output power decreases with increasing module surface temperature as in case of monocrystalline PV modules (-0.48%/C). This is essential in the case of Trimo EcoSolar PV modules, because module surface temperature is higher, since they are glued to a sandwich panel with insulation on the underside.

- Small weight (7.7 kg) and thickness (3 mm) of the PV module: no additional reinforcement of roof and breakthroughs and architectural appearance of the building were not changed.

- A special cell structure (three layers of silicon) that allows the exploitation of a wider spectrum of light and a lower sensitivity to partial shading (each cell has a bypass diode), which is quite pronounced in the MFE TEB 1 due to the surrounding buildings (cooling tower, stacks of GT units PB4 and PB5, etc.).
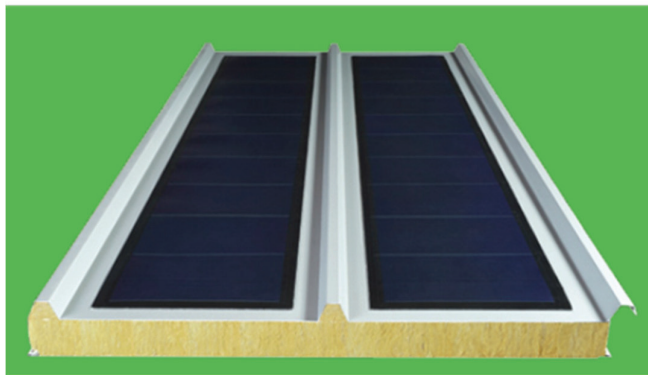
Figure 1: Trimo EcoSolar PV sandwich panel

Basic technical data of the MFE TEB 1 are listed in Table 1. Location is shown in Figure 2a.

2.2   Photovoltaic system MFE TEB 2

At the end of 2009, we began the construction of a parking lot, the roof of which was made with PV modules. In this case, PV modules simultaneously perform the functions of the roof and the photovoltaic system. This is a so-called integrated photovoltaic system, named MFE TEB 2.

The parking lot's roof is designed as a metal construction made of hot zinc profiles with a roof made of monocrystalline PV modules. The roof has a distinct design, which is carried out in such a way that in case of rain, water does not pass through the slots between the PV modules. The problem of "sealing" was solved by a combination of omega profiles and channels, which form a catching rainwater catchment system under the PV modules. With this solution, we avoided the use of standard sealing solutions, which are expensive and intended for larger sloping roof angles (usually from a 22° angle forward). Another distinct feature of the parking lot's roof is that it can be upgraded during its lifetime so that electric cars could be powered.

We finished with the construction of a photovoltaic system MFE TEB 2 at the end of March 2010 and started with trial run in April 2, 2010. Basic technical data of the MFE TEB 2 are listed in Table 1. Location is shown in Figure 2b.

2.3   Photovoltaic system MFE TEB 3

Simultaneously to the construction of the photovoltaic system MFE TEB 2, we started with construction of the photovoltaic system MFE TEB 3, located on the roof of the GT units PB4 and PB5.

With the construction of MFE TEB 3, we approached to the ideal installation of the photovoltaic system (azimuth south, inclination 7°), but there we encountered the problem of partial shading of the surrounding artificial barriers (stacks of GT units PB 1-3, lightning rod, etc.). Due to this problem, it was necessary to thoughtfully implement strings of the PV modules and choose an appropriate configuration of the inverters, which significantly eliminated the effect of partial shading.

Figure 2: Photovoltaic systems MFE TEB 1-3

We finished the construction of the photovoltaic system MFE TEB 3 at the end of March 2010 and started the trial run in April 2, 2009. Basic technical data of the MFE TEB 3 are listed in Table 1. Location is shown in Figure 2c.

Table 1: Basic technical data of the photovoltaic systems MFE TEB 1-3

		MFE TEB 1		MFE TEB 2		MFE TEB 3	
Nominal power [kW$_p$]		38.08		81.78		49.9	
Location		Business building		Car parking roof		Roof of GT unit PB 4 in 5	
Inclination angle [°]		5 °		5 °		7 °	
Azimuth angle [°]		90° (E), 180° (S), 270° (W)		90° (E)		180° (S)	
Year of construction		2009		2010		2010	
PV modules	Type	PVL 136		Asola 290 W/72		Solarwatt M230	
	Material of solar cell	Amorphous Si		Monocrystall. Si		Monocrystall. Si	
	Nom. power P_{mpp} [W]	136		290		235	
	Efficiency [%]	6 %		15 %		15 %	
	Manufacturer	Unisolar (USA)		Asola (DE)		Solarwatt (DE)	
	Dimensions [mm]	5486×394×4		1979×990×50		1610×1060×50	
	Weight [kg]	7.7		26.6		24	
	U_{mpp} [V] $\quad$ I_{mpp} [A]	33	4.1	37,44	7,83	47,8	4,9
	U_0 [V] $\quad$ I_{sc} [A]	46.2	5.1	44,71	8,38	59,1	5,4
	Temper. coeff. of output power [%/°C]	-0.21		-0.48		-0.50	
	No. of PV modules	280		282		212	
	Effective surface of solar cells [m²]	524		564		339	
	Specific power of PV module [W/m²]	73		145		147	
Inverters (No. x kW)		SMA (2×3 and 6×5) 1 phase		SMA (6×11 and 3×5) 1 phase		SMA (1×5, 2×7 and 3×11) 1 phase	
Average annual energy produced [kWh]		34,278		74,290		45,266	
Average annual energy yield [kWh/kW$_p$]		900		908		906	

3   PERFORMANCE RATIO AND ENERGY YIELD

Performance ratio is the ratio between the actual energy and theoretical energy produced by a photovoltaic system. It is defined in IEC 61724, *[8]*, and shows the proportion of energy that is available for transmission to the network after deducting lost energy (due to thermal losses, conductivity losses, inverter losses, mismatch between components, dustiness of PV modules, shading losses, system degradation, snow on modules, system failure, etc.). Performance ratio is calculated by (3.1):

$$PR = \frac{E}{E_{sim}} = \frac{E}{\sum \eta_{STC} \cdot H_c \cdot \Delta t \cdot A}$$

(3.1)

Where *PR* is performance ratio, *E* [kWh] is the actual energy produced, E_{sim} [kWh] theoretical energy produced, η_{STC} [%] efficiency of PV modules at standard test conditions (STC), H_c [kW/m^2] solar radiation on tilted surface, Δt [h] time of operation and *A* [m^2] effective surface of PV modules.

Energy yield describes the relationship between the energy produced and the nominal power of a photovoltaic system and is calculated by (3.2):

$$Y = \frac{E}{P_{STC}}$$

(3.2)

Where *Y* [kWh/kW$_p$] is the energy yield, *E* [kWh] actual energy produced, and P_{STC} [kW] is the nominal power of the photovoltaic system. Energy yield represents the number of hours that the photovoltaic system would need to operate at its nominal power to provide the same energy. The unit of *Y* could be also kWh/kWp. Energy yield depends on solar radiation and temperature.

4   RESULTS

The analysis of the performance ratio and the energy yield is calculated based on the operating data of the photovoltaic systems MFE TEB 1-3 for a six-year period (2011–2016). During this time, photovoltaic systems operated steadily, stable and without long interruptions or failures.

Energy production data were obtained from distribution network operator database (SODO). In these data, the losses on the AC side (such as losses in the connecting cable between the AC switch block and the connection measuring block (PMO)) are taken into account. Solar radiation data were obtained from local communication units (SMA Sunny Webbox), which are part of every photovoltaic system. Each communication unit has its own solar irradiation sensor, surface temperature sensor and ambient temperature gauge. The values of solar irradiation enabled us to calculate the performance ratio for each photovoltaic system. The following analyses were carried out:

- Analysis of the PR according to (3.1) for the average of six years in the period from 2011 to 2016.
- Analysis of the Y according to (3.2) for the average of six years in the period from 2011 to 2016.
- Analysis of the PR according to (3.1) for each year in the period from 2011 to 2016.
- Analysis of the Y according to (3.2) for each year in the period from 2011 to 2016.

In Table 2, average monthly values of PR and Y are presented for photovoltaic systems MFE TEB 1-3 during the period from 2011 to 2016. In Table 3, average annual values of PR and Y values are presented for photovoltaic systems MFE TEB 1-3 for each year, during the period from 2011 to 2016.

Table 2: Average monthly values of PR and Y for photovoltaic systems MFE TEB 1-3 in the period from 2011-2016

Month	MFE TEB 1		MFE TEB 2		MFE TEB 3	
	PR [%]	Y [kWh/kW$_p$]	PR [%]	Y [kWh/ kW$_p$]	PR [%]	Y [kWh/ kW$_p$]
Jan	0.64	18.66	0.74	20.84	0.58	20.64
Feb	0.62	22.83	0.74	27.87	0.58	25.03
Mar	0.92	70.52	0.84	74.95	0.72	75.79
Apr	0.99	100.77	0.85	102.80	0.74	101.12
May	0.92	122.05	0.78	120.89	0.70	120.96
Jun	0.94	129.68	0.78	128.13	0.71	129.97
Jul	0.86	130.10	0.76	134.30	0.67	132.85
Aug	0.90	126.80	0.73	120.68	0.66	121.63
Sep	0.97	84.35	0.76	82.05	0.66	79.87
Oct	0.92	50.99	0.77	50.28	0.68	50.92
Nov	0.89	24.62	0.79	25.69	0.69	25.50
Dec	0.75	18.77	0.71	19.94	0.63	21.23
Average	**0.86**	**75.01**	**0.77**	**75.70**	**0.67**	**75.46**
Sum		**900**		**908**		**906**

Table 3: Average annual values of PR and Y for photovoltaic systems MFE TEB 1-3 in the period from 2011-2016

	2011		2012		2013	
	PR [%]	Y [kWh/kW$_p$]	PR [%]	Y [kWh/kW$_p$]	PR [%]	Y [kWh/kW$_p$]
MFE TEB 1	0.93	999.42	0.84	1000.58	0.75	829.12
MFE TEB 2	0.77	1012.21	0.76	968.94	0.81	855.86
MFE TEB 3	0.72	990.28	0.68	986.27	0.67	841.23
	2014		2015		2016	
	PR [%]	Y [kWh/kW$_p$]	PR [%]	Y [kWh/kW$_p$]	PR [%]	Y [kWh/kW$_p$]
MFE TEB 1	0.81	764.08	0.84	897.40	0.97	910.32
MFE TEB 2	0.83	904.44	0.78	864.06	0.71	844.97
MFE TEB 3	0.67	857.65	0.62	887.14	0.63	870.47

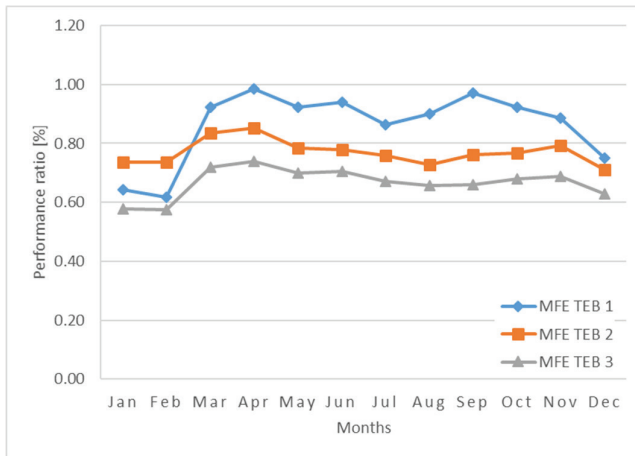The data in Tables 2 and 3 are graphically shown in Figures 3 to 6.

Figure 3: *Average monthly values of PR for photovoltaic systems MFE TEB 1-3 in the period from 2011-2016*

Figure 3 shows that PR of photovoltaic systems MFE TEB 1, 2 and 3 in January, February and March is significantly lower in comparison to the summer months. The lower values of the PR in these months are the result of the accumulation of snow on PV modules, due to the low inclination angles of the PV modules of all three photovoltaic systems.

Figure 3 shows that the PR of the MFE TEB 1 is significantly higher in spring, summer, and the early autumn months than the PR of MFE TEB 2 and MFE TEB 3. This can be explained due to the better solar cells on MFE TEB 1 (amorphous silicon) than on MFE TEB 2 and 3 (monocrystalline silicon). Monocrystalline silicon solar cells have a significantly higher temperature coefficient of efficiency or output power than amorphous silicon solar cells do, which can be seen in Table 1.
Figure 3 shows that the PR of MFE TEB 2 is significantly higher than that of MFE TEB 3, although MFE TEB 3 has a better inclination and azimuth angle (7°, 180° - south) than MFE TEB 2 (5 °,90° - east). This can be explained by the significantly larger partial shading at MFE TEB 3 throughout the year (stacks of GT units PB1-3, lightning rods, discharge pipes on the roof of the GT units PB4, 5) and poor cooling of PV modules. Partial shading is also present at MFE TEB 1 but, due to the by-pass diode on each cell, the effect is not noticeable.

Table 2 and Figure 4 show the average monthly values of *Y* for photovoltaic systems MFE TEB1, 2 and 3 in the period from 2011-2016. The results show that due to low inclination angles, inconvenient azimuths angles, and the presence of partial shading, the energy yield is lower than in the case of optimal conditions. The Y of all three photovoltaic systems is almost the same throughout all months, which can also be seen in Figure 4.

Photovoltaic system MFE TEB 2 reaches the maximum average value of Y in the period from 2011-2016, due to the relatively low presence of partial shading (compared with MFE TEB 1 and MFE TEB 3) and good cooling conditions of PV modules.
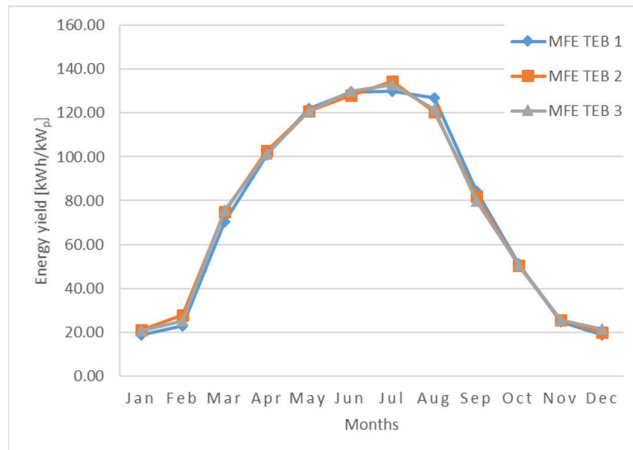
Figure 4: *Average monthly values of Y for photovoltaic systems MFE TEB 1-3 in the period from 2011-2016*

Figure 5 shows the average annual values of the PR for solar photovoltaic systems MFE TEB 1-3 and the average annual value of solar irradiation for the period from 2011 to 2016. Figure 5 shows that in the case of higher solar irradiance (2011, 2012, 2015, and 2016), photovoltaic system MFE TEB 1 reaches higher values of PR than photovoltaic systems MFE TEB 2 and MFE TEB 3, due to lower temperature coefficient of efficiency or output power of solar cells but in the case of lower solar irradiance (2013, 2014) the impact of the temperature coefficient is not so great.

Figure 5 shows that the annual PR of the photovoltaic system MFE TEB 3 shows slightly lower values in the observed period, than that from photovoltaic system MFE TEB 2, due to the presence of partial shading. Photovoltaic systems MFE TEB 2 and 3 show no major deviations. The presence of partial shading at the MFE TEB 3 reflected in the course of the annual PR, which is slightly lower than that of the MFE TEB 2 within complete observed period. In contrast, in the course of MFE TEB 2 and 3 there are no major deviations.
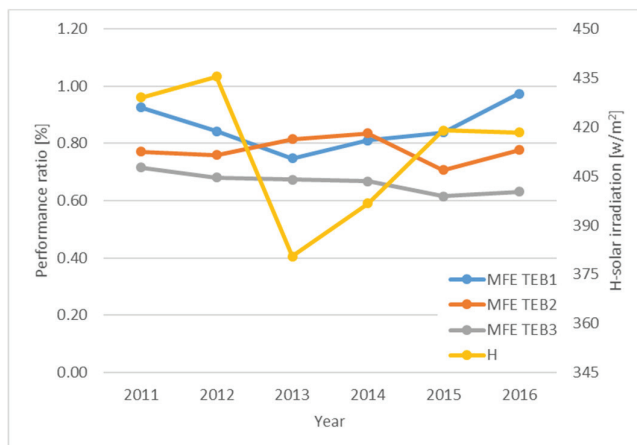
Figure 5: *Average annual values of PR for photovoltaic systems MFE TEB 1-3*
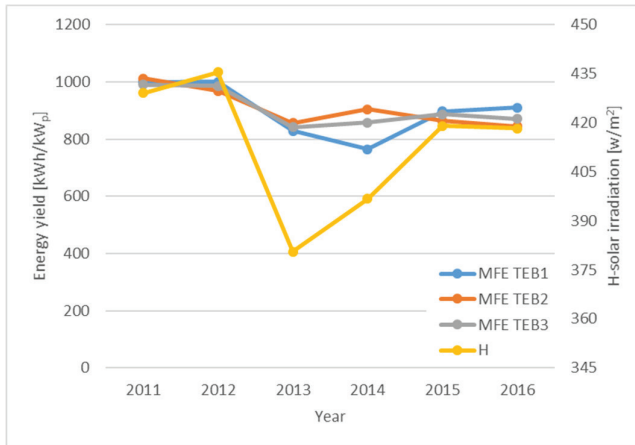
Figure 6: Average annual values of Y for photovoltaic systems MFE TEB 1-3

Figure 6 shows the average annual values of Y for photovoltaic system MFE TEB 1-3 and the average annual value of solar irradiation for the period from 2011 to 2016. Figure 6 shows that photovoltaic system MFE TEB 1 has the lowest Y in 2013 and 2014, due to lower solar irradiation. This confirms the fact that the lower temperature coefficient of efficiency or output power at lower values of solar irradiation no longer contribute to a higher Y.

5   CONCLUSION

In this paper, the analysis of the PR and Y of photovoltaic systems MFE TEB 1-3 is presented, based on operational and meteorological data for the period from 2011 to 2016. The results show that values of PR and Y are lower than in the case of optimal conditions, due to inconvenient inclination and azimuth angles, the presence of partial shadings and snow barriers.

The results confirm the fact that the efficiency factors for amorphous silicon solar cells have lower temperature coefficients of efficiency or output power than monocrystalline silicon solar cells do; in the summer months or the periods of higher intensity of solar irradiation these levels are higher in comparison to those of monocrystalline silicon solar cells. Based on the results of the fourth chapter, we conclude that this applies to the average annual values of solar irradiation, which exceed 410 W/m².

PV modules of MFE TEB 1 are glued on thermally insulated roof sandwich panels, which reduces the heat exchange and causes significantly higher surface temperature of the PV module, even at lower solar irradiation. The effect of lower temperature coefficient is most pronounced at higher values of solar irradiation and higher ambient temperature.

References

[1]   **S. Seme, K. Sredenšek, B. Štumberger, M. Hadžiselimović:** *Photovoltaic systems in Slovenia and performance ratios : a review*. V: KROPE, Jurij (ur.), et al. Renewable energy sources : (conference proceedings), Maribor: University of Maribor Press: Faculty of Chemistry and Chemical Engineering, 2017, str. 303-313, doi: 10.18690/978-961-286-061-5.19

[2]   **S. SEME, K. Sredenšek, Z. Praunseis, B. Štumberger, M. Hadžiselimović:** *Optimal price of electricity of solar power plants and small hydro power plants: technical and economical part of investments*, Energy, ISSN 0360-5442. 2018 vol. 157, str. 87-95

[3]   **S. Seme, N. Lukač, B. Štumberger, M. Hadžiselimović:** *Power quality experimental analysis of grid-connected photovoltaic systems in urban distribution networks*, Energy, ISSN 0360-5442. 2017, vol. 139, str. 1261-1266

[4]   **S. Seme, G. Srpčič, D. Kavšek, S. Božičnik, T. Letnik, Z. Praunseis, B. Štumberger, M. Hadžiselimović:** *Dual-axis photovoltaic tracking system : design and experimental investigation,* Energy, ISSN 0360-5442. maj 2017, vol. 139, str. 1267-1274

[5]   **S. Seme, B. Štumberger, M. Hadžiselimović:** *A novel prediction algorithm for solar angles using second derivative of the energy for photovoltaic sun tracking purposes,* Solar energy, ISSN 0038-092X, nov. 2016, vol. 137, str. 201-211

[6]   **S. Seme, J. Požun, B. Štumberger, M. Hadžiselimović:** *Energy production of different types and orientations of photovoltaic systems under outdoor conditions,* Journal of solar energy engineering : Transactions of the ASME, ISSN 0199-6231, 2015, vol. 137, issue 2, str. 021021-1 - 021021-10

[7]   **K. Sredenšek:** *Energetska učinkovitost in tehnično-ekonomska analiza investicije sončnih elektrarn po Sloveniji*, magistrsko delo, 2017

[8]   IEC 61724 "*Photovoltaic system performance monitoring – Guidelines for measurement, data exchange and analysis*" 2017

Nomenclature

TEB	Thermal power plant Brestanica
PV module	Photovoltaic module
RES	Renewable energy sources
MFE	Mala fotovoltaična elektrarna – small photovoltaic power plant
CCIS	Chamber of Commerce and Industry of Slovenia
GT	Gas turbine
PB	Plinski blok – gas turbine unit
PR	Performance ratio
Y	Energy yield
STC	Standard test conditions
E	Actual energy produced
E_{sim}	Simulated energy produces
η_{STC}	Efficiency of solar module at STC
H_c	Solar irradiation
Δt	Operating time of photovoltaic system
A	Active surface of solar module
P_{STC}	Nominal power of solar module at STC

ROOT WELD METAL IMPACT TOUGHNESS OF AN ENERGY COMPONENT

UDARNA ŽILAVOST V KORENU ZVARA ENERGETSKE KOMPONENTE

Julijan Salamunić[R]

Keywords: steel, root weld metal, impact toughness, welded joints

Abstract

In energy engineering, high-strength low-alloy steels are used for building high-loaded modern constructions. The weakest link of a welded structure is a welded joint at which cracks appear, which can lead to sudden destruction. Thus, the welded joints are made with a high impact toughness that can prevent unstable crack propagation.

This research deals with the experimental determination and analysis of Charpy impact toughness curves at the weld root of an energy component for different additive materials.

Povzetek

V energetiki uporabljamo visokotrdnostna malolegirana konstrukcijska jekla za gradnjo visoko obremenjenih modernih konstrukcij. Najšibkejši člen varjene konstrukcije je zvarni spoj v katerem se pojavljajo razpoke, ki lahko povzročijo nenadno porušitev. Zaradi navedenega gradimo zvarne spoje tako, da imajo zvari visoko udarno žilavost, ki lahko zadržijo nestabilno širjenje razpok.

V raziskavi je predstavljena eksperimentalna določitev in analiza krivulj Charpyjeve udarne žilavosti v korenu zvara energetske komponente za različne dodajne materiale.

[R] Corresponding author: Ph.D. Student, Julijan Salamunić, Faculty of Energy Technology, University of Maribor, Tel.: +386 (0)3-7770-400, Mailing address: Koroška cesta 62a, Velenje, Slovenia, E-mail address: julko.julko@gmail.com

1   INTRODUCTION

A welded joint is a critical part of any welded construction because with the introduction of heat into the base material (BM) during welding the mechanical properties of the base material (the construction steel) can be worsened A welded joint consists of a weld and on both sides the so-called heat affected areas (HAA). There are two types of welded joints: joints where the weld strength is lower than the base material. Such joints are called low-strength welded joints. The so-called high-strength welded joints occur when we build a weld material with a higher yield strength than the base material has. It is known that the high-strength low-alloy (HSLA) steels are problematic for welding which means that they require a specially prescribed welding technology. Most often such steels are welded by preheating and with smaller energy inputs in a way that we make a multi-welded weld connection with thinner wedges. Moreover, cracks endanger the safety of the entire weld construction because they can cause a collapse due to a sudden overload. That is why a welded joint has to have good mechanical properties, the most important of which is the impact toughness which is determined experimentally with the standard dynamic Charpy test. Most errors, while welding of HSLA steel, occur during and after the welding, namely at the weld root, which is the critical point of a welded joint and must have a high impact toughness. Due to the above, it is extremely important that prior to building a high strength construction, we must test the welded joints that are welded with various additive materials [1-5].

This article examines HSLA steel of strength class SC 50, of the manufacturer Železarna Jesenice and the additive materials of Elektroda Jesenice. The welded joints are welded with eight different additive materials in such a way that they form a low-strength welded joint. The impact toughness of the weld root is determined with the standard dynamic Charpy test. The analyses of the whole curve of impact toughness are given with the emphasis on the part of the curve that shows the lowest impact toughness: the so-called brittle area of the curve. For the root part of the weld, the microstructures are determined [7-8]

2   MATERIALS AND MECHANICAL PROPERTIES

We chose the improved HSLA steel Niomol 490K, strength class 50 and 40mm thick, from the Slovene manufacturer Acroni Jesenice, for the welding of the high-strength welded joint. Welding took place at the company Goršek d.o.o., Šentjanž. The steel was not preheated since we decided to weld with low-strength additive materials that have a lower limit of flow than the base material; that is why preheating was not necessary, which also reduces the costs of the production of welded joints. The heat input was 15kJ/cm of the weld; the cooling time was $\Delta t8/5$ = 9s.

The X welding form was suitable for welding, and the result of a multi-welded X weld joint can be seen in Figure 1.

Figure 1: X form of a multi-welded weld joint

A lower strength weld was welded with eight various additive materials:

- welding wire VAC 60 and VAC 65
- coated basic electrode EVB 50 and EVB 55
- coated basic electrode EVB Ni and EVB S
- filled wire Filtub 28B
- coated basic electrode EVB NiMo.

Mechanical properties of the base material and the additive materials are given in Table 1.

Table 1: Mechanical properties of the base material and the additive materials

Welded joint Additive materials/BM	R_p [MPa]	R_m [MPa]	A_{gt} [%]	E [GPa]	n
VAC 60/Niomol	475	564	13.43	210	0.144422
VAC 65/Niomol	488	597	13.54	211	0.140573
EVB 50/Niomol	511	603	12.52	221	0.134246
EVB 55/Niomol	501	578	12.33	205	0.136926
EVB S/Niomol	432	555	15.68	208	0.158796
EVB Ni/Niomol	563	676	11.73	210	0.121847
EVB NiMo/Niomol	535	686	12.86	207	0.128224
Filtub 28 B/Niomol	537	625	11.79	209	0.127746
Base material NIOMOL 490K	606	680	10.03	201	0.113201

Here are the basic characteristics of the additive materials:

VAC 60: Coppered welding wire/welding rod according to MAG procedure. It is suitable for welding of non-alloy steels and low-alloy steel up to 530 Mpa. It is used for welding of boiler plates, pipes, steels for shipbuilding, micro-alloy steels and steel castings. VAC 60 was tested according to the CTOD method.

VAC 65: Coppered welding wire/welding rod according to MAG procedure. The content of Si and Mn is slightly higher than in VAC 60; therefore, the yield strength and the strength of the solid weld are also higher. The increased level of Si also reduces the sensitivity to surface impurities and provides a smooth weld. It is suitable for the welding of non-alloy steels and low alloy steel up to 640 Mpa. It is used for welding of boiler plates, pipes, steels for shipbuilding, micro-alloy steels, and steel castings. VAC 65 was tested according to the CTOD method.

EVB 50: Basic, CTOD-tested electrode for welding of non-alloy and low-alloy steels and steel castings up to 610 Mpa, as well as for welding of fine-grained steels with increased strength. Welds are tough even at low temperatures and resistant to cracks. The content of hydrogen is lower than 5 ml/100g of the weld. The electrode has excellent welding properties and a stable arc. The slag can be easily removed. It has 118% efficiency. The strength of the welding current in different positions does not necessarily need to be changed.

EVB 55: Basic, CTOD-tested electrode, especially suitable for welding of low-alloy steels and carbon steels containing up to 0.6% of carbon. The welds are resistant to hot-cracking and have a low content of dissolved hydrogen, as well as high toughness even at low temperatures and aging resistance. The electrode has very good welding properties; slag can be removed easily and with minimal spraying.

EVB S: Double-coated basic, CTOD-tested electrode with very good welding properties in forced positions. The electrode has a very stable arc. It is suitable for the welding of root welds with direct and alternating current.

EVB Ni: With Ni alloyed, basic, CTOD-tested electrode for the welding of non-alloy and low alloy steels up to 685 Mpa and fine-grained steel with limits up to 800 Mpa and with guaranteed mechanical properties at low temperatures. The weld toughness at low temperatures is very good.

EVB Ni-Mo: With Ni and Mo alloyed, a basic electrode for welding of steels with increased resistance to atmospheric corrosion and for welding of fine-grained steels with limits up to 460 Mpa

Filtub 28B: High-frequency firing wire, CTOD-tested, alloyed with Mn, Ni, and Mo, suitable for welding fine-grained steels of tensile strength up to 750 Mpa. Welding with this wire shows excellent mechanical properties at low temperatures, minimal spraying at welding, smooth surface of the weld and easy slag removal.

3 EXPERIMENTAL PROCEDURE

The Charpy test is thoroughly described in Chapter 3. Charpy samples were taken from the weld root as shown in Figure 2.
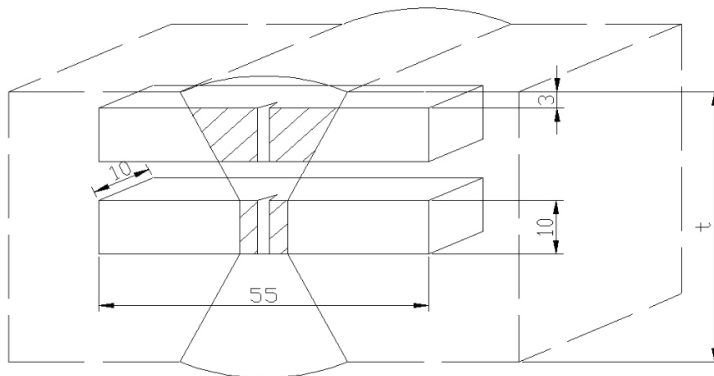
Figure 2: *The removal of Charpy samples from the weld root; the possible removal of samples from the cap of the weld are indicated*

The Charpy experiment was carried out at temperatures of -60, -50, -40, -30, -20, -10, 0, +10, and +20 ℃, in which three test samples were prepared for each test temperature. The results of impact toughness in tabular form are shown in Table 2 [8-11].

Figure 3: *The appearance of the manufactured and broken Charpy samples*

Figure 4: *The appearance of the groundbreaking surface of the Charpy sample*

Table 2: *The results of impact toughness for additive materials EVB 55, EVB NiMo, Filtub 28B, EVB Ni, EVB 50, EVB S, VAC 65 and VAC 60*

EVB 55

Temp-60	-50	-40	-30	-20	-10	0	10	20
72	78	86	88	108	112	123	160	165
80	88	99	78	78	128	140	151	140
64	62	70	110	99	96	80	95	129
						114.333 3	135.333 3	144.666 7
72	76	85	92	95	112			

FILTUB 28B

Temp-60	-50	-40	-30	-20	-10	0	10	20
50	64	61	74	80	61	91	119	121
42	94	50	59	89	95	58	142	81
71	47	70	96	40	122	120	79	100
54.3333 3	68.3333 3	60.3333 3	76.3333 3	69.6666 7	92.6666 7	89.6666 7	113..333 3	100.666 7

EVB Ni

Temp-60	-50	-40	-30	-20	-10	0	10	20
62	76	71	88	69	79	92	100	110
48	96	59	78	81	61	115	138	129
33	60	62	91	88	25	62	172	185
47.6666 7	77.3333 3	64	85.6666 7	79.3333 3	55	89.6666 7	136.666 7	141.333 3

EVB 50

Temp-60	-50	-40	-30	-20	-10	0	10	20
31	50	68	80	94	105	118	131	178
42	62	58	71	81	138	158	185	199
47	46	42	65	64	81	75	172	101
40	52.6666 7	56	72	79.6666 7	108	117	162.666 7	159.333 3

EVB S

Temp-60	-50	-40	-30	-20	-10	0	10	20
25	32	39	46	56	85	82	108	134
38	38	45	58	71	100	115	138	165
30	19	30	35	31	63	91	75	95
31	29.6666 7	38	46.3333 3	52.6666 7	82.6666 7	96	107	131.333 3

VAC 65

Temp-60	-50	-40	-30	-20	-10	0	10	20
35	41	49	55	79	84	90	115	121
47	49	53	65	100	110	121	91	143
21	31	29	42	41	61	141	151	181
34,33333	40.33333	43.66667	54	73.33333	85	117.3333	119	148.3333

VAC 60

Temp-60	-50	-40	-30	-20	-10	0	10	20
32	42	54	62	65	90	110	130	121
38	48	65	85	105	128	141	161	143
30	20	50	31	75	78	61	100	165
33-33333	36.66667	56.33333	59.33333	81.66667	98.66667	104	130.3333	143

EVB Ni-Mo

Temp-60	-50	-40	-30	-20	-10	0	10	20
48	61	63	69	83	90	101	125	142
37	55	46	74	61	71	82	93	132
30	50	59	81	75	86	94	110	137
38.33333	55.33333	56	74.66667	73	82.33333	92.33333	109.3333	137

At each test, temperature mean values were calculated,through which the polynomial approximation was carried out to obtain a smooth curve of impact toughness. The curves of impact toughness for additive materials EVB 55, EVB NiMo, Filtub 28B, EVB Ni, EVB 50, EVB S, VAC 65, and VAC 60 are shown in Figure 5.
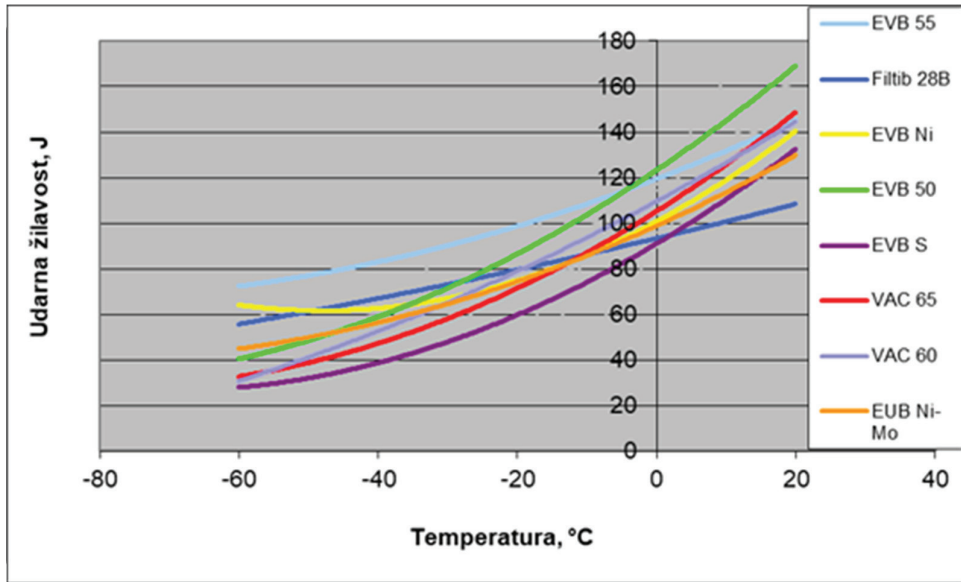
Figure 5: *The curves of impact toughness at the weld root for additive materials EVB 55, EVB NiMo, Filtub 28B, EVB Ni, EVB 50, EVB S, VAC 65, and VAC 60*

4   ANALYSIS OF RESULTS

The classification of impact toughness curves in the weld root for additive materials EVB 55, EVB NiMo, Filtub 28B, EVB Ni, EVB 50, EVB S, VAC 65 and VAC 60 is shown in Figure 2. There we can see that the curves are not evenly distributed, but they intersect each other. This finding shows the complexity of the problem of determining impact toughness in welded compounds which are highly heterogeneous microstructures.

The highest impact toughness can be seen in the weld that was welded with the EVB 55 electrode, in the temperature range from -60 ℃ to – 5 ℃, and the lowest impact toughness in the weld that was welded with the EVB S electrode in the temperature range from -60 ℃ to +5 ℃. All eight curves of impact toughness in the temperature range from -40 ℃ to +20 ℃ exceeded 28 J for fracture, which indicates that the toughness of all eight welds is sufficient for the construction of welded joints with the required welding technology on the field.

Only the curve of impact toughness for the weld that was welded with the EVB S electrode for the temperature range from -60 ℃ to -40 ℃ did not exceed the minimum required toughness of 28 J. Good toughness at lowest temperatures is the most important.

Thus, as we can see from the distribution of the curves for the impact toughness that in the temperature range from -60 ℃ to -20 ℃ the weld made with the EVB S electrode has the lowest toughness (but still higher than 28 J), Followed by welds made with electrodes VAC 65, VAC 60, EVB 50, and Filtub 28B. The highest impact toughness is with the weld made with the EVB 55 electrode.

From the distribution of the curves of impact toughness, we can see that the curve of impact toughness for the weld made with the EVB Ni electrode has strikingly high growth, namely in the

temperature range from -60 ℃ to -40 ℃ where it has a higher impact toughness at -60 ℃ than at -40 ℃. We should look for the cause of this anomaly in the actual location of the notch. It is certain that in the case of higher toughness at the lower temperature of -60 ℃ the notch was placed in the tougher bainite microstructure of the weld, whereas in the case of lower toughness at -40 ℃ the notch was placed in a more brittle coarse-grained ferrite-bainite microstructure of the weld.

Precisely because of the aforementioned problem of notch placement, we did a metallographic survey of microstructures that appeared after welding at the root of the hardened weld and are shown in Figures 3-6. Figure 1 shows the most favourable and toughest microstructure of the base material, Niomol 490-K steel. Fine-grained bainite microstructure at the weld root is the cause for attaining the highest impact toughness of the weld made with the EVB 55 electrode. Moreover, in contrast, the reason for the lowest impact toughness for the weld made with the EVB S electrode was the less tough coarse-grained ferrite microstructure.

Due to the anticipated construction of lower strength welds, a micro-hardness test at the weld root of all eight welded joints was performed. The distribution of hardness inequality coefficients at the weld root that was welded with additive materials EVB 55, EVB NiMo, Filtub 28B, EVB Ni, EVB 50, EVB S, VAC 65, and VAC 60 (Figure 1-8) proves that, even after welding, all weld roots showed a factor of hardness inequality M lower than 1, which means that all actual weld roots are in the low-hardness area. With this finding, the prescribed welding technology is confirmed as the correct one.

5   CONCLUSIONS

The Charpy impact test is a standardized impact toughness test and is carried out with the Charpy hammer. It is mandatory for the construction of pressure vessels (reactors, pipelines, reservoirs, etc.) and other complex welded constructions in the energy sector.

The stiffly lower weld was welded with eight different additive materials: welding wires VAC 60 and VAC 65, coated basic electrodes EVB 50 and EVB 55, coated basic electrodes EVB Ni and EVB S, filled wire Filtub 28B and coated basic electrode EVB NiMo.

The highest impact toughness was seen in the weld root made with the EVB 55, in the temperature range from -60 ℃ to +5 ℃. All eight curves of impact toughness, at the temperature range from -40 ℃ to +20 ℃, exceeded the energy of 28 J for fracture, which indicates that the toughness of all eight welds is good enough for making welded joints on an actual construction with the prescribed welding technology. Good toughness at negative/lower temperatures is the most important.

Due to the complexity of determining impact toughness in an extremely heterogeneous weld root, an analysis of microstructures in the weld root and base material is necessary. It was carried out with an optical microscope and according to the classification of end microstructures in the hardened weld (International Institute of Welding). Metallographic research showed two key microstructures, the so-called fine-grained bainite microstructure and coarse-grained ferrite microstructure. Some weld roots contained a mixed ferrite-bainite microstructure.

The distribution of the hardness inequality coefficients at the weld root welded with additive materials EVB 55, EVB NiMo, Filtub 28B, EVB Ni, EVB 50, EVB S, VAC 65, and VAC 60 (Figure 1-8) proves that, even after welding, all weld roots showed a factor of hardness inequality M lower

than 1, which means that all actual weld roots are in the low-hardness area. With this finding, the prescribed welding technology is confirmed as the correct one. In practice, this means that we can make such welds without using preheating, which strongly reduces the costs of making an welded joint.

References

[1]   **Z. Praunseis.:** Zapiski predavanj pri predmetu Optimiranje oskrbovalnih sistemov, Fakulteta za Energetiko, 2013

[2]   EN-875.: Standard method of Charpy Impact Toughness Test, London,1993

[3]   **Z. Praunseis, J. Avsec.:** Gradniki v energetiki, Fakulteta za energetiko, Univerzitetni učbenik, 2011

[4]   **Z. Praunseis.:** Vpliv znižane trdnosti strjenega zvara z vključenimi heterogenimi področji na lomne lastnosti zvarnega spoja visokotrdnostnega jekla, Univerza v Mariboru, Doktorska disertacija, 1998

[5]   **N. Gubeljak.:** Celovitost konstrukcij, Univerza v Mariboru, Znanstvena monografija, 2006

[7]   **H. Granjon.:** Metalurške osnove varjenja, Zveza društev za varilno tehniko Slovenije, Ljubljana, 1994

[8]   http://sl.wikipedia.org/wiki/SlikeNiko

[9]   http://sl.wikipedia.org/commons4746kerbschlagbiegeversuchMachine.jp

[10]   **K. Easterling.:** Introduction to the Physical metallurgy of Welding, Butterworths, London etc., 1983

[11]   http://lotric-certificiranje.si/laboratoriji/laboratorij-za-kovine-mehanske-preiskave-in-mikroskopijo/preskusi-udarne-zilavosti-na-preskusancih/ (2015)

MECHANICAL TESTING OF HETEROGENEOUS ENERGY COMPONENTS

MEHANSKO PREIZKUŠANJE HETEROGENIH ENERGETSKIH COMPONENT

Tadej Pavlin[R]

Abstract

Welding of a high-strength low-alloyed (HSLA) steel with the aim to produce an under-matched weld joint presents a technological challenge for modern welded structure production. Attention should be paid to the level of strength mismatching, which should provide sufficient toughness of the weld metal by using an appropriate welding consumable (wire, electrode) and welding procedure. High toughness of weld metal is necessary to enable local plastic deformation and to prevent brittle fracture. It is of utmost importance to exclude the possibility of plane faults (hydrogen cracking, lack of fusion, etc.) and local-brittle-zone (LBZ) appearance in HSLA steel under-matched welded joints, which can cause failure.

This research aimed to estimate the weld metal Crack Tip Opening Displacement (CTOD) fracture toughness using standard procedures for three differently under-matched welded joints.

[R] Corresponding author: Ph.D. Student, Tadej Pavlin, Faculty of Energy Technology, University of Maribor, Tel.: +386 (0)3-7770-400, Mailing address: Koroška cesta 62a, Velenje, Slovenia, E-mail address: tadej.pavlin@livar.si

Povzetek

Varjenje visokokakovostnega nizko legiranega jekla (HSLA) z namenom izdelave nizkotrdnostnega zvarnega spoja predstavlja tehnološki izziv za moderno izdelavo varjene konstrukcije. Pri tem moramo upoštevati stopnjo trdnostne neenakosti, ki naj bi zagotovila zadostno žilavost jeklenega zvara z uporabo ustrezne varilne žice (žice, elektrode) in postopka varjenja. Visoka žilavost jeklenega zvara je potrebna, da se omogoči lokalna plastična deformacija in prepreči krhki lom. Zelo pomembno je, da se izključi možnost ravninskih napak (vodikova razpokljivost, pomanjkanje fuzije itd.) in oblika lokalnega krhkega območja (LBZ) v visokotrdnostnih (HSLA) jeklenih zvarih, kar lahko povzroči zlom. Namen te raziskave je bil oceniti lomno žilavost jeklenih zvarov s CTOD preizkušanjem za tri različne nizkotrdnostne zvarne spoje.

1   INTRODUCTION

Welding of a high-strength low-alloyed (HSLA) steel to produce an under-matched weld joint presents a technological challenge for current welded structure production. When the yield strength is lower in weld metal than in base metal, the welded joint is under-matched. The strength mismatch factor (M) is defined as the ratio of weld-metal to base-metal yield strengths so that M < 1 defines an under-matched welded joint. Under-matched welded joints are used for the repair welding of joints damaged during hard hydrogen cracking without pre-heating, especially for welded joints made of HSLA steels operation conditions or by short period overloading. They are also recommended to prevent cold cracking with yield strength above 700 MPa. Specifically, HSLA steels usually require pre-heating if matching or overmatching welding consumable is used, which is not only expensive but also needs a carefully designed and strictly followed welding procedure. Finally, there is a frequent need for additional thermal or mechanical treatment afterwards.

One should pay attention to the level of strength mismatching, which should provide sufficient toughness of the weld metal by using an appropriate welding consumable (wire, electrode) and welding procedure. The high toughness of weld metal is necessary to enable local plastic deformation and to prevent brittle fracture. It is of utmost importance to exclude the possibility of plane faults (hydrogen cracking, lack of fusion, etc.) and local-brittle-zone (LBZ) appearance in HSLA steel under-matched welded joints, which can cause failure, *[1-7]*.

This research aimed at estimating the weld metal CTOD fracture toughness for three differently under-matched welded joints.

2   MATERIALS AND MECHANICAL PROPERTIES

High-strength low-alloyed (HSLA) steel in a quenched and tempered condition, corresponding to the grade HT 80, was used. The Fluxo Cored Arc Welding process (FCAW) was used, and two different tubular wires were selected. Three different types of global under-matched welded joint were produced: one homogeneous and two heterogeneous. The homogeneous welded joint was made with pre-heating and post-heating of the base material, entirely with the same consumable (wire WELTEC B 575). Two different types of heterogeneous welded joints were made using a softer consumable (wire WELTEC B 370) for the soft root layer (one with two and the other with four passes) in order to avoid pre-heating of the base material and to prevent cold cracking. The

filler passes were made with the wire WELTEC B 575 as well as the cap passes. Chemical compositions of the base metal and all-weld metals are given in Table 2.1.

Weld metal mechanical properties were determined by round tensile specimens extracted from the root and the filler region of X-groove welds in the weld direction. The expected mechanical properties of homogeneous and heterogeneous under-matched welded joints have not been reached neither in the filler region nor in the root region, as shown in Tables 2.2 and 3.1. The cause was weld metal alloying with elements from the diluted base metal.

The alloying effect was more pronounced in the root region than in the filler region, and it was also the main reason for local strength mismatch appearing in the thickness and direction of homogeneous and heterogeneous welds (see chemical analysis given in Tables 2.1. and 3.1.).

Table 2.1: Chemical composition of base material and all-weld metals

Chemical composition [%]	C	Si	Mn	P	S	Cr	Ni	Mo	Cu	Al
HT 80	0.16	0.68	0.75	0.020	0.003	0.79	0.09	0.032	0.24	0.037
WELTEC B 575	0.05	0.04	1.52	0.011	0.008	0.08	1.45	0.66	-	-
WELTEC B 370 soft root	0.05	0.25	0.61	0.011	0.008	0.06	0.07	0.03	-	-

Table 2.2: Mechanical properties of base material and all-weld metals

Designation	Rp [MPa]	Rm [MPa]	Elongation [%]	Charpy toughness [J]	Expected M
HT 80	710	810	15.5	85, 91, 100 at 0 °C	-
WELTEC B 575	542	591	23	47, 70, 71 at -40 °C	0.76
WELTEC B 370 soft root	403	466	32	100, 215, 145 at -40 °C	0.56

Bearing in mind the values of strength mismatch factors M in Table 3.1, one can see that the root inhomogeneous weld metal is overmatched (M = 1.05 => 5% overmatching), which leads to strongly increased cold-cracking susceptibility, whereas the filler region has practically the same strength as the base material (M = 0.99). This effect proves the concept of heterogeneous weld in an under-matched joint with two-pass (M = 0.81 => 19% undermatching) or four-pass (M = 0.91 => 9% undermatching) soft root layer in order to prevent cold cracking without pre-heating of the base material.

3   EXPERIMENTAL PROCEDURE

The set of B × B specimens was taken from under-matched homogeneous and heterogeneous welds to obtain fracture behaviour of welded joints with defects like cold cracks and lack of fusion, which often exist in real welded joints. With CTOD testing of welded joints, they are treated as

planar (plane) faults. Thus, in the CTOD specimen, the surface cracks with different depths were positioned in weld metal with the aim of locating the fatigue-crack-tip front in different microstructure regions of mismatched welded joints and of analysing the material behaviour at the crack tip in regard to the nearby microstructure influence.

Fracture toughness of homogeneous and heterogeneous under-matched welded joints was evaluated using the standard static CTOD test at GKSS Research Center Geesthacht in Germany, *[2]*. Specimen loading was carried out with constant crosshead speed v = 0.5 mm/min. The test temperature was -10 °C according to the recommendation of the OMAE (Offshore Mechanics and Arctic Engineering) association. For CTOD testing, the single specimen method was used by BS 7448, *[1]*. To evaluate fracture toughness of under-matched welded joints, standard single-edge notched-bend (SENB) specimens (B × B, B = 36 mm) with surface notches in the weld metal were used, as shown in Table 3.2.

The B × B specimens were fatigue pre-cracked from the surface to a distinct welded joint microstructure.

Table 3.1: *Mechanical properties and chemical composition of homogeneous and heterogeneous under-matched weld joints*

Designation	Rp [MPa]	Rm [MPa]	Elongation [%]	Charpy V [J] at -10 °C	Expected *M*	Achieved *M*
Base material						
HT 80	693	830	19.6	79, 78, 64	-	-
Heterogeneous weld joint – filler material WELTEC B 575						
WM – cap	687	804	22.3	110, 104, 102	0.76	0.99
WM – root	730	803	21.8	72, 38, 50	0.76	1.05
Heterogeneous weld joint – filler material WELTEC B 370 in the root (the rest WELTEC B 575)						
WM – 2 x soft root passes	567	625	19.7	-	0.56 at the root	0.81 at the root
WM – 4 x soft root passes	631	673	21.9	35, 17, 34	0.56 at the root	0.91 at the root

Composition [%]										
	C	Si	Mn	P	S	Cr	Ni	Mo	Cu	Al, Ti, Nb
WM hom. – cap	0.04	0.44	1.48	0.009	0.003	0.12	1.63	0.49	0.12	-
WM hom. – root	0.10	0.33	0.89	0.011	0.008	0.73	1.11	0.42	0.13	-
WM – 2 x soft passes	0.12	0.41	0.78	0.011	0.006	0.40	0.10	0.17	0.16	-
WM – 4 x soft passes	0.10	0.33	0.78	0.012	0.007	0.24	0.13	0.11	0.13	-

Table 3.2: *Fatigue crack positioning in SENB specimens (B x B) at under-matched weld joints*

Weld groove width 2H (at the crack tip)	Fatigue crack position	Crack depth [*a/ W*]
	↓ CAP	
2H = 14.1 mm		~ 0.25
	↓ + 2 mm above soft root	
2H = 13.9 mm	h2	~ 0.25
	↓ in the soft root	
2H = 6.8 mm	h1	~ 0.48
	↓ in the soft root	
2H = 7.4 mm	h2	~ 0.43

For all specimens, the fatigue pre-cracking was carried out with the GKSS Step-Wise High R ratio method (SHR) procedure. During the CTOD tests, the DC potential drop technique was used for stable crack-growth monitoring. The load line displacement (LLD) was also measured with a reference bar to minimize the effects of possible indentations of the rollers. The CTOD values were directly measured by specially developed δ5 clip gauge (Figure 3.1.) on the specimen side surfaces at the fatigue crack tip over a gauge length of 5 mm.

3.1   Fractographic and metallographic examinations

To determine the influence of crack-tip microstructure on fracture behaviour, the metallographic and fractographic examinations were performed. For fractographic examinations, the Scanning Electronic Microscope (SEM) was used, while the metallographic investigations were performed by the Optical Light Microscope. After fractographic examinations, the specimens were cut in crack-growth direction and polished and etched with 3% Nital.
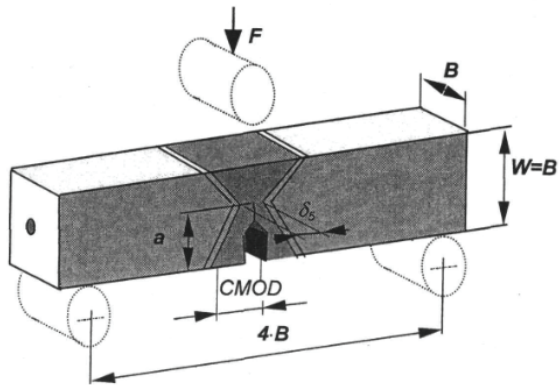
Figure 3.1: *Three-point specimen (B × B) and measuring points (CMOD, δ₅)*
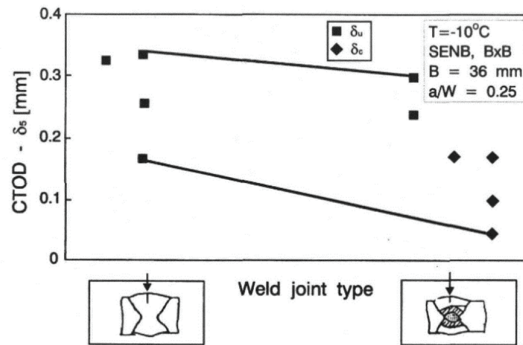

Figure 3.2: *Weld metal CTOD fracture toughness of homogeneous and heterogeneous under-matched weld joint*
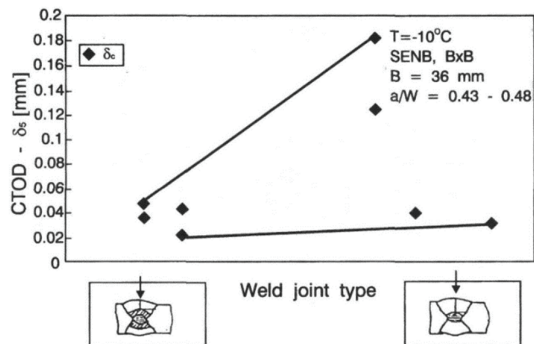

Figure 3.3: *Soft root layer CTOD fracture toughness of heterogeneous under-matched weld joints*

At low magnification, the fracture surfaces of each type of specimen exhibited different fracture surfaces, strongly affected by the type of the welded joint region.

4   ANALYSIS OF RESULTS

The results of CTOD fracture toughness of B × B specimens with surface cracks in under-matched homogeneous and heterogeneous welds are shown in Figures. 3.2 and 3.3. As a consequence of different crack depths (a/W), different constraints act at the crack tip, significantly influencing the CTOD fracture toughness values. Therefore, only the comparison of CTOD values obtained using specimens with the same crack depth is reasonable. Average crack depths a/W are given in Table 3.2 for a set of specimens.

The influence of soft root layer on fracture toughness of filler passes (WELTEC B 575) in heterogeneous weld metal is noticeable from the comparison of CTOD values obtained using specimens with surface cracks (a/W = 0.25) positioned in filler passes of homogeneous and heterogeneous weld (Figure 3.2). The fracture toughness was higher for specimens with surface cracks in filler passes of the homogeneous weld than for specimens with surface cracks in filler passes of the heterogeneous weld.

After initial stable crack growth (δu – Figure 3.2 and Figure 4.1 - fracture and cross-section M-M), in all CTOD specimens from homogeneous weld, brittle fracture has occurred when crack tip (Figure 4.1. - cross-section M-M and detail A) reached LBZ, i.e. low toughness bainitic microstructure (Figure 4.1. - detail B) with precipitated Fe3C at boundaries of M-A phases (Figure 4.2.), as was proven with the appearance of significant pop-in and arrested brittle fracture (Figure 4.1. - fracture and cross-section M-M).

Hardness increase (~ 340 HV) at the crack tip was noticeable (Figure 4.1. - detail B), as a consequence of material strengthening just before brittle fracture occurred.

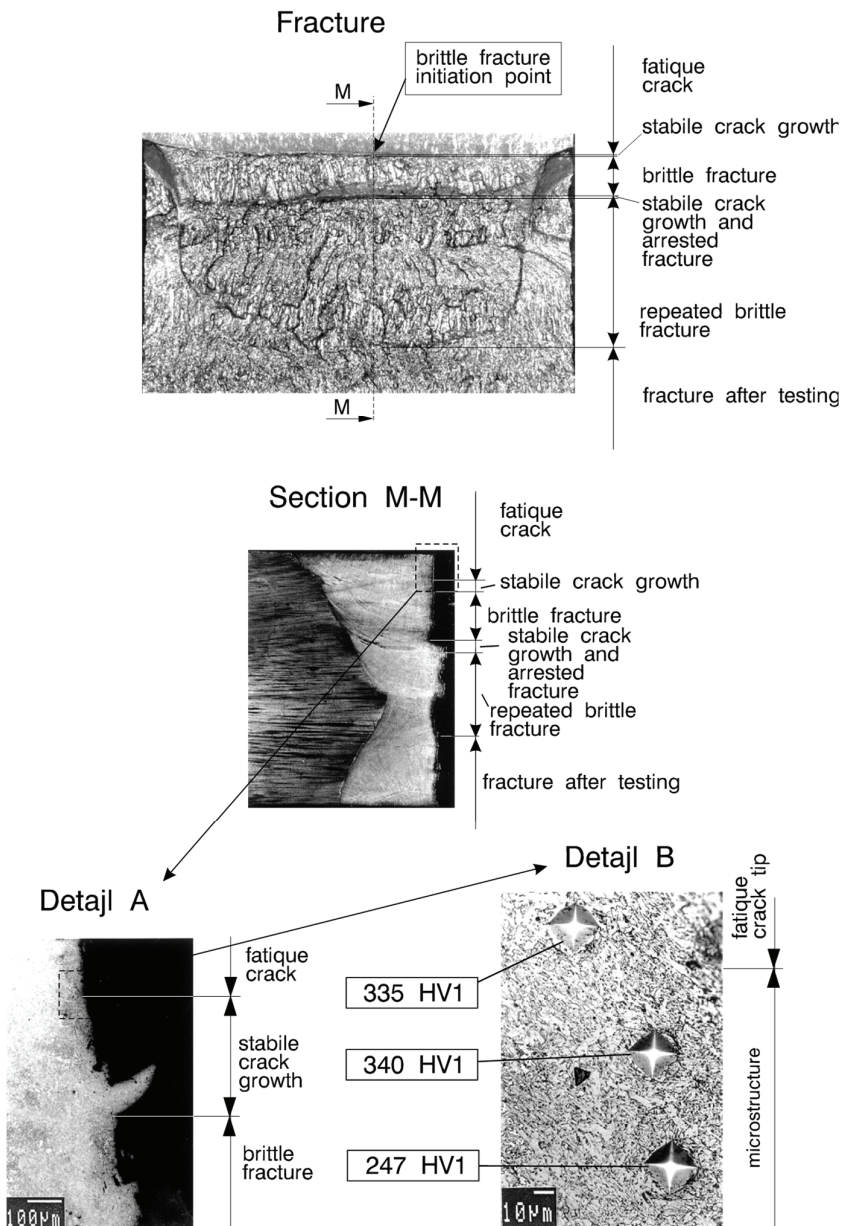**Figure 4.1:** *Fracture and microstructure in the vicinity of brittle fracture initiation point of specimen B × B with surface crack (a/ W = 0.25) in filler region of homogeneous weld. Near the brittle fracture initiation, point a bainitic microstructure (Detail ~ A) is visible, and at higher magnification (Detail - B) contours of primary ferrite (PF) can be seen, formed at primary γ grains*
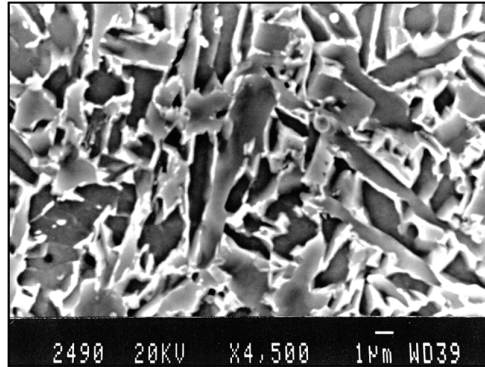
Figure 4.2: *Bainitic microstructure with precipitated Fe₃C at M-A phase boundary in the weld metal of the homogeneous welded joint*

To analyse the effect of soft root layers on fracture toughness of filler passes and also of heterogeneous welds as a whole, it was necessary to locate the fatigue crack so that it gradually approaches the soft root layer (Table 3.2). From the comparison of CTOD results (Figures. 3.2 and 3.3), the effect of crack depth a/W and weld width 2H (Table 3.2) on CTOD fracture toughness is clear, being the lowest for the specimens with deep crack (a/W~ 0.5) in soft root layer, where the weld width 2H is the smallest. The effect of constraint on fracture toughness is also noticeable from the comparison of the curves F-CTOD, where it is clear that the final instabilities and higher CTOD values have appeared at higher forces and for specimens with shorter cracks, where the crack tip was located approximately 2 mm above the soft root layer (Figure 4.3. - cross-section N-N and detail A). This was not only a consequence of the remaining ligament W - a and the effect of weld groove width, 2H, on the CTOD values, but also a consequence of the beneficial effect of bainitic microstructure at the fatigue crack tip, which directly reflects the fracture toughness values. Because of that, the final fracture of specimens with the crack positioned close to the soft root layer appeared after prior stable crack growth (Figure 4.3. – detail A) through the tougher bainitic microstructure (Figure 4.3. - detail B) of filler passes, when the crack tip reached the soft root layer.

The soft-root-layer low toughness was determined by Charpy impact V testing (Table 3.1.). The main cause for low soft-root-layer toughness was a change of microstructure of all-weld metal obtained by wire WELTEC B 370, which was exposed to different alloying mechanisms during welding in the root region. Specifically, the all-weld metal microstructure of soft root weld metal was bainitic, having high toughness, but because of the above-mentioned reasons, its microstructure was changed to harmful ferritic microstructure (Figure 4.4. - detail B), causing low toughness of soft root layer.
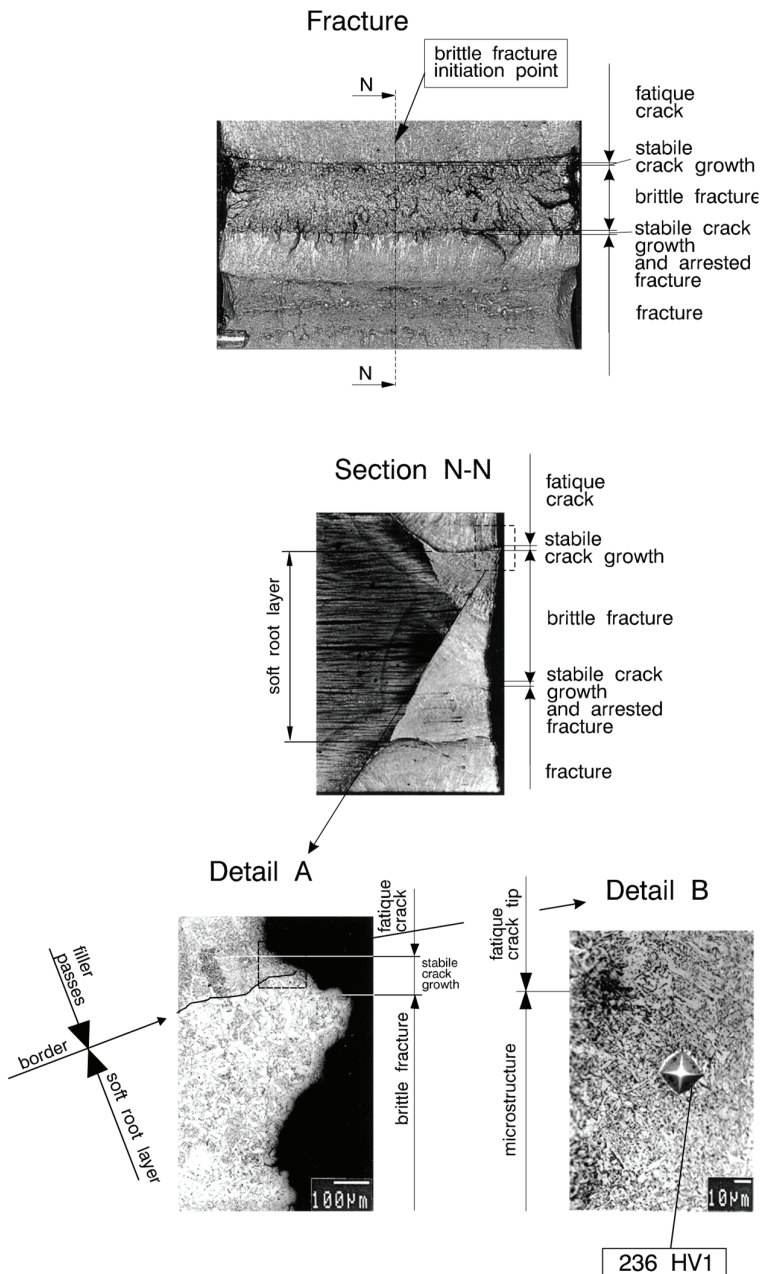
Figure 4.3: *Appearance of fracture surface and evaluation of microstructure at fatigue crack tip in specimen B × B with surface crack (a / W = 0.43) close to the boundary of soft root region. Bainitic microstructure at fatigue crack tip can be seen (Detail - A). At higher magnification (Detail - B), contours of primary ferrite (PF) are visible, formed on primary γ grains*

Figure 4.4: Fracture and microstructure near the brittle fracture initiation point of specimen B x B with fatigue crack (a / W = 0.48) positioned in soft root region. Ferritic-bainitic microstructure of soft root weld metal (Detail - A) is visible with distributed brittle M-A constituents along ferrite grain boundaries (Detail - B)

Figure 4.5: *Resistance (R) curves for specimens (B × B) with surface crack (a/ W = 0.43)*
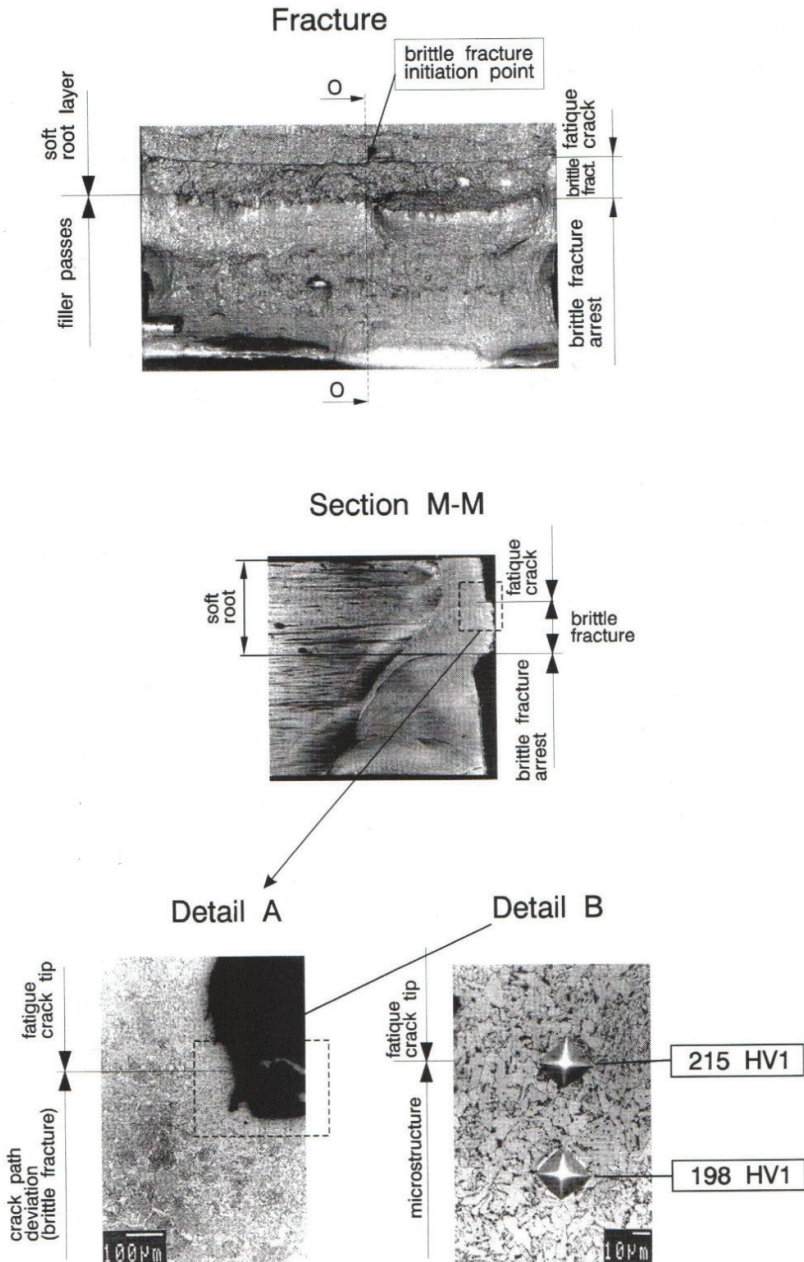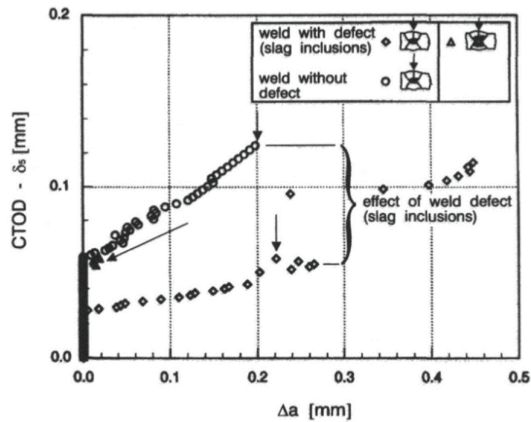*in soft root layer*

The brittle fracture has appeared due to low fracture toughness of the soft root layer, being especially emphasized for specimens with the fatigue crack directly positioned in the soft root layer (Figure 4.4. - cross-section O-O and detail A), where such brittle fracture appeared (without prior stable crack growth) and finally arrested in the tougher filler region with beneficial bainitic microstructures (Figure 4.3. - cross-section N-N and detail B). The CTOD values of the soft root layer were additionally reduced because of constraint, being largest in the soft root layer of these specimens, because the crack depth (a/W was the largest, weld groove shape coefficient 2H/W - a the smallest, and heterogeneity the most prominent). Comparison of CTOD fracture toughness results (Figure 3.2) shows a significant influence of the soft root layer on the fracture toughness of filler region (WELTEC B 575) in heterogeneous welds, causing weld metal fracture toughness to be much higher for the specimens with a surface crack (a/W = 0.25) in the homogeneous weld than in a heterogeneous one. The results of CTOD fracture toughness (Figure 3.3.) for specimens with surface cracks (a/W = 0.43-0.48) in the two-passes and four-passes soft root layer indicate somewhat higher toughness of the former one.

From Figure 4.5, the influence of defects (slag inclusion) on fracture toughness of two-pass soft root layer can be observed, because the fatigue crack tip was positioned in it, causing premature specimen fracture and thus low fracture toughness of soft root layer.

The most frequent brittle-fracture initiation points of specimens with crack-tip positions in the soft root layer were Al-Si-Mn inclusions (Figure 4.6.) and TiCN carbides. The reason for low fracture toughness of soft root layer is the already mentioned microstructure modification due to the alloying effect of base metal.
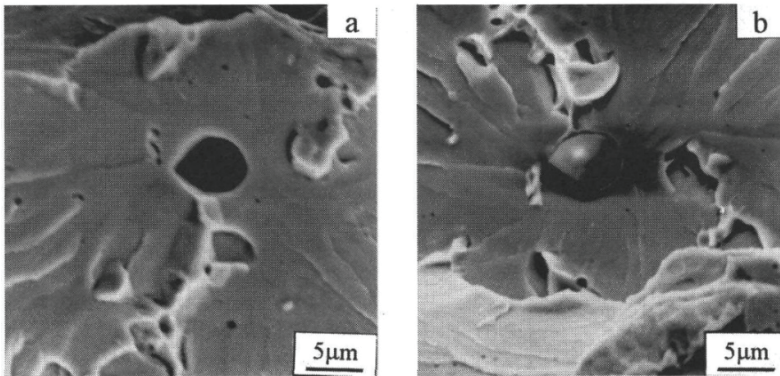
Figure 4.6: *Appearance of brittle fracture initiation point (Al-Si-Mn inclusion) on left a) and right b) fracture surface of specimen B × B with surface crack in the heterogeneous weld, indicated by EDX analysis*

5   CONCLUSIONS

The selection of soft tough weld consumable (wire) does not guarantee tough root layer in the under-matched weld. The improper selection of weld consumable and thermal effects of subsequent passes on soft root layer can cause modification of the microstructure and reduction of its toughness. Weld metal CTOD fracture toughness, measured by surface notched B × B specimens with homogeneous and heterogeneous weld metal, is higher for the homogeneous weld. Weld metal CTOD fracture toughness for the heterogeneous weld decreases as the soft root volume increases.

Fracture behaviour of CTOD specimens with surface cracks depends on the following three parameters: geometrical constraint due to the different crack depth a/W, groove shape coefficient 2H/(W − a), and local plastic constraint in the root region of the weld joint, due to strength mismatching. For the CTOD testing of heterogeneous welded joints, specimens with surface cracks starting from the surface and directed toward weld thickness should be used.

References

[1]   BS 5762, Methods for crack opening displacement (COD) testing, The British Standards Institution, London 1979

[2]   ASTM E 1152-87, Standard test method for determining J-R curves, Annual Book of ASTM Standards, Vol. 03.01, American Society for Testing and Materials, Philadelphia, 1990

[3]   ASTM E 1290-91, Standard test method for crack-tip opening displacement (CTOD) fracture toughness measurement, American Society for Testing and Materials, Philadelphia, 1991

[4]   GKSS Forschungszentrum Geesthacht GMBH, GKSS-Displacement Gauge Systems for Applications in Fracture Mechanic

[5]   **Z. Praunseis, M. Toyoda, T**. **Sundararajan**: *Fracture behaviours of fracture toughness testing specimens with metallurgical heterogeneity along crack front*, Steel res., 71, Vol. 9, 2000

[6]   **Z. Praunseis, T**. **Pavlin**: *Mehansko preizkušanje jeklenih zvarov za procesno industrijo, študija projekta*, Fakulteta za energetiko, 2016

[7]   **T. Sundararajan, Z**. **Praunseis**: *The effect of nitrogen-ion implantation on the corrosion resistance of titanium in comparison with oxygen- and argon-ion implantations*. Mater. tehnol., Vol. 38, Iss. ½, 2004

RESEARCH IN VIRTUAL ENGINEERING

RAZISKAVE V VIRTUALNEM INŽENIRINGU

Gorazd Hren[R], Marko Pezdevšek[1]

Keywords: Virtual Engineering, Rapid Prototyping, Virtual Reality

Abstract

Virtual reality systems and 3D printing have achieved an adequate level of development to be considered in innovative applications in education and research. One of the challenges of this technology is the associated costs, which have been unaffordable for educational and research institutes. However, in recent years, computer hardware and software accompanied by the development of printing technology has made it more feasible for teaching strategies. From the research point of view, it is time for companies to innovate by incorporating new technologies, particularly those that inject products with greater intelligence and the ability to monitor, learn, and fix problems while functioning in their virtual environment.

Povzetek

Sistemi navidezna resničnosti in tehnologije 3D tiskanja so dosegle zadostno stopnjo razvoja, da jih je potrebno upoštevati in vpeljati kot inovativne aplikacije na področju izobraževanja in raziskovanja. Enega večjih izzivov te visoke tehnologije predstavljajo stroški nabave in vzdrževanja, ki so izredno visoki za izobraževalno raziskovalne ustanove. V zadnjih letih je razvoj teh tehnologij in s tem nižanje stroškov dosegel nivo, ko jih je mogoče vključiti v prihodnje strategije poučevanja in raziskovalnega dela. Iz raziskovalnega vidika, je čas, da podjetja za evalvacijo inovacij vključujejo nove tehnologije, še posebej tiste, ki omogočajo razvoj izdelkov z višjo dodano vrednostjo in omogočajo večje spremljanje, učenje in odpravljanje težav izdelkov, med obratovanjem v njihovem navideznem delovnem okolju.

[R] Gorazd Hren, Tel.: +386 6202218, Mailing address: University of Maribor, Faculty of Energy Technology, Hočevarjev trg 1, 7280 Krško, E-mail address: gorazd.hren@um.si

[1] University of Maribor, Faculty of Energy Technology

1   INTRODUCTION

In research and education, new technologies are a highly influential factor, much more than ever before. A generation of engineering students is entering higher education with significant computing knowledge, and with higher expectations that academic institutes will introduce them to appropriate technologies for their successful entry into industry. Research in virtual reality has the potential for expansion in the coming years. In the research by IEEE Transmitter, *[1]*, over 150,000 attendees of the Consumer Electronics Show produce the eight top technological trends that should be tracked. Virtual Reality (VR) and Rapid Prototyping (RP) are on the 4th and 7th places, respectively. In recent years, VR systems have received much attention from researchers and industry. Recent advances in hardware and software have brought this technology within reach of researchers at universities and in industry. As a concept, VR has been around for over forty years and is characterised by high degrees of immersion and interaction. Its main goal is to make users believe that they are actually in the computer-operated environment. A VR system has the potential to create systematic human testing, training, and treatment environments, which allow the control of complex, immersive, dynamic 3D simulated presentations. This, in turn, makes the interaction sophisticated and enables the tracking of behaviour and the recording of performance possible. VR can be identified with the following concepts: simulation, interaction, artificiality, immersion and network communication. VR implementations make use of high-speed and high-quality 3D graphics and audio with a combination of interactive devices to achieve realism and believability.

The use of this technology is spreading throughout industry, providing the ability to virtually explore a complete product before conception, to improve techniques in the process of product development using CAD software, and to validate a design before committing to making a physical prototype (Figure 1).

Figure 1: Development of product design in CAD to VR

3D printing (3DP) as part of RP is a potent tool for the design and manufacturing industries. With the rapid development of 3DP technologies in recent years, the equipment has become more affordable and accessible to the public. 3DP has been used in research and manufacturing and is used in engineering education to enhance design-related courses. Over the years, it has gradually become an essential component of the design and manufacturing curricula from first-year design and drafting courses to final-year projects. The main reason that RP has become so popular in engineering education is the simplicity of its operation, compared to traditional machining processes, and the spontaneous delivery of results, which provides a significant

impact on the experience. From the literature (e.g. Sinha, *[2]*), it has been observed that RP is helpful in visualization, presenting real-world applications, and closing the gap between theories and practices. These designs involve complex geometric structures that are difficult to fabricate using traditional machining processes. With RP, the prototypes can be fabricated easily, and the projects can be completed within reasonable timeframes and budget ranges. In addition to ease of use, the freeform capability and recently available multi-material processes open new possibilities for engineering practices and some other areas.

2   PRINTING IN 3D

The Laboratory of Virtual Engineering at the Faculty of Energy Technology of the University of Maribor is equipped with two small devices and one large format state-of-the-art 3D printing device.

3DSYSTEMS CubePro Trio (Figure 2) measures 20 × 23 × 27 cm; three different materials in a single print job can be used with an accuracy of 0.3 mm. The most commonly used materials are ABS (Acrylonitrile Butadiene Styrene), a common thermoplastic known for its use in injection moulding; PLA (Polylactic Acid), a popular biodegradable thermoplastic derived from renewable resources, such as corn starch, used for many applications; and nylon, when an object requires both strength and a small amount of flexibility. The printing process is extended with another input device: iSense scanner (Figure 2) that can scan volumes of 0.2-3.0 m^3 in VGA resolution (640x480) and accuracy up to 1 mm. All equipment is from a single provider and used integrated software solutions.

Figure 2: 3DSYSTEMS CubePro Trio and CUBE iSense scanner

TYPE A MACHINES (Figure 3) has built size of 30 × 30 × 30 cm with an accuracy of 0.2 mm and uses different materials, including PLA, ABS, INGUS, and nylon. It has its own software for optimisation of printing.

Figure 3: Type A Machines Series 1 and corresponding software

Figure 4: Wind turbine CAD model, blade 3D print and turbine measurements in wind tunnel

Figure 4 presents different stages in the wind turbine blade development, CAD model, printed blade, and picture from measurements in the wind tunnel.

EnvisionTec XEDE (Figure 5) is a state-of-the-art large-format 3D printer with a size of 46 × 46 × 46cm and accuracy of 0.05mm. The material must be 3SP photopolymers. The printer is equipped with well-known Magics software to prepare geometry and its own software to optimize printing processes on an onboard computer.

EnvisionTEC's Xede 3SP large-format 3D printer enables the production of exceptionally large 3D parts, at fast build speeds without sacrificing surface quality and part accuracy. The Xede 3SP uses EnvisionTEC's 3SP (Scan, Spin and Selectively Photocure) technology to quickly 3D print highly accurate parts from STL regardless of geometric complexity. The 3D printer is delivered and installed with all the relevant software to enable the automatic generation of supports and perfect model production. The reliability of the light source and the high-speed productivity of the Xede 3SP makes it one of the most competitive 3D printers on the market. Figure 5 shows the same very small and highly accurate printed parts and the blade of winter turbine from the same CAD model in Figure 4.
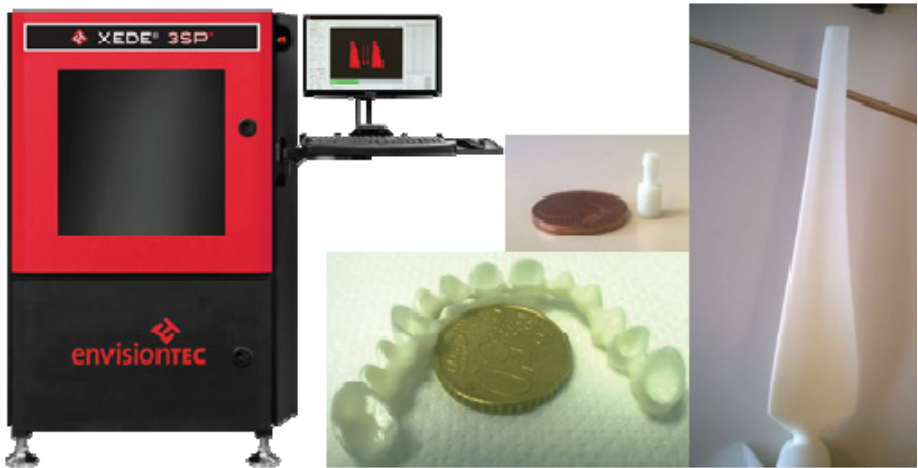
Figure 5: *EnvisionTEC XEDE and some small parts produced*

3   VISUALISATION IN 3D

The Laboratory of Virtual Engineering at the Faculty of Energy Technology has recently been equipped with technologies for VR to improve and enrich the research and, of course, educational work. Significant computing power and graphical user devices and interfaces were installed.

The Corner Cave Vario 90/180 is a flexible 3D Projection System. There are two options to use it. The first case is a double-sized Powerwall, and the second case is like a two-sided cave, as seen in Figure 6.

Two individual Powerwalls to make this possible. Each measures 3.2 × 2.0 m with WQXGA (2560 x 1600) resolution and has 5000-lumen brightness. Each Powerwall is mounted to its chassis. The chassis is mounted behind the projection surface and are on rollers to make it moveable.

Figure 6: *Big Powerwall or Two-Sided Cave (3Dims, 2017)*

The projectors are mounted to an overhang in front of the projection surface. A BARCO F50 WQXGA Projector enables high-quality projections at small distances from the screen (Figure 7).
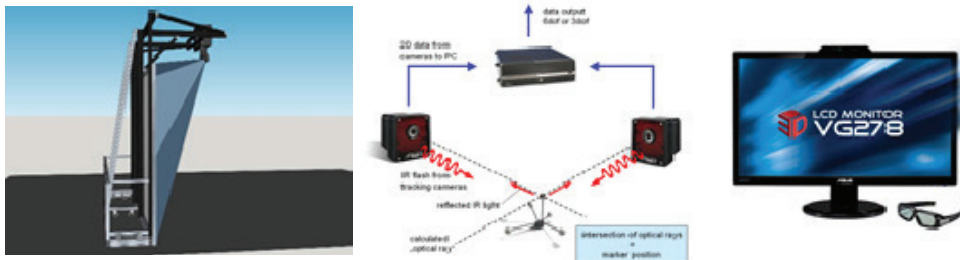

Figure 7: Projection distance, motion tracking system and 3DVision (VRLogic; nvidia.com)

The laboratory is equipped with three 4K resolution monitors enabling to work stereo 3D on a computer monitor with NVIDIA 3DVision equipment on 200Hz (Figure 7).

Such powerful computer graphics are supported by two workstations, each with following main specifications:

- Intel Dual Socket Motherboard
- 2× Intel® Xeon E5_2699v3, 18 cores 2,3GHz (Haswell) main onboard CPUs
- 128 GB DDR4 RAM
- 400GB SSD, 2TB HDD
- Nvidia Quadro M6000, Nvidia Tesla K40 12GB 2880 CUDA Cores,
- Intel X450 Dual 10GBase.

Other equipment is needed for work interactively in a virtual environment. We use an ART Trackpac4 System with four cameras as the tracking system (Figure 7) of movement in the working area with an ART controller, targeting shutter glasses and wand (Figure 8).

Figure 8: Interaction devices: Wand, Master Shutter glasses and 3D SpaceMouse

P3D Virtual Sight (VRLogic, 2017) is a virtual reality software solution designed for the visualization of digital aspect mock-ups at a 1:1 scale on multi-screen immersive systems. Visualization on a 1:1 scale makes it possible to assess objects with regard to their actual size and complements the photorealistic rendering quality of the Lumiscaphe (2017) rendering engine with an extra dimension of realism. P3D Virtual Sight conforms to a wide range of configurations. It is suitable for various visualisation profiles and modes, such as multi-screen

devices, image walls based on juxtaposed projections, immersive systems of the CAVE type or Head Mounted Displays.

P3D Virtual Sight (Figure 9) also supports multiple stereoscopic display modes and can be interfaced with various tracking systems to enhance sensorial experimentation during project review.

Figure 9: VR pilot software on monitor and in corner cave

For modelling and geometry creation, the laboratory is equipped with CATIA, SolidWorks, and Ansys software for advanced numerical analysis as could be seen in Figure 10.
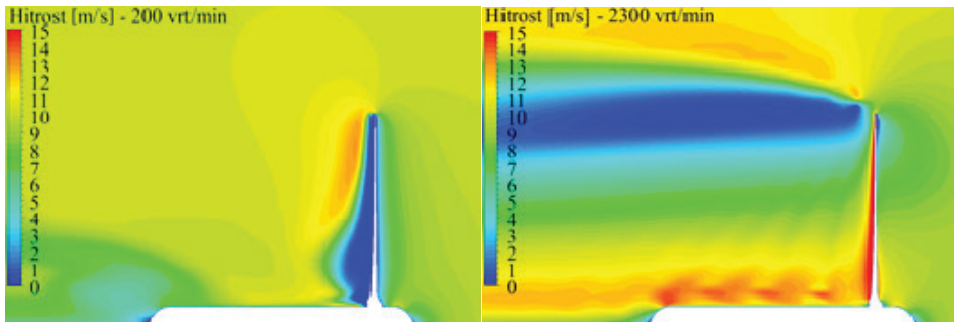
Figure 10: Results of numerical analysis of wind turbine from Figure 4

4   CONCLUSION

Interactive and immersive 3D visualisation virtual reality technology and rapid prototyping are ubiquitous in research institutes and in industry and will have a profound impact on research and manufacturing processes in future. These technologies represent a tool that can create a pipeline for cooperation and research with industry and prepare the next generation of graduate engineering with the required skills. While cost is recognised as a key challenge, leading institutes have already implemented the technology for research and education purposes. However, the more the technology advances, the more affordable it becomes. Thus, it is expected that institutes will implement the necessary hardware and software level for virtual reality and rapid prototyping to be strategically adopted in the future of engineering.

References

[1]   IEEE Transmitter, 8 Tech trends that should be track in 2016, [http://transmitter.ieee.org/8-tech-trends-track-2016/] April 7, 2017

[2]   **A. Sinha**: *New Frontiers in Manufacturing Education: Rapid Prototyping, 3D Scanning and Reverse Engineering*, Proceedings of 2009 ASEE Southeast Section Conference, 2009

[3]   **A. G. Abulrub, A. N. Attridge, M. A. Williams**: *Virtual Reality in Engineering Education, The Future of Creative Learning*, 2011 IEEE Global Engineering Education Conference (EDUCON), Jordan, 2010

[4]   3Dims.de, Available: www.3dims.de/news (April 7, 2017)

[5]   VRLOGIC, Available: www.vrlogic.com (April 7, 2017)

[6]   envisionTEC, Available: http://envisiontec.com/3d-printers/large-frame-family/xede-3sp/ (April 7, 2017)

[7]   3DSYSTEMS, CubePro, Available: http://www.3dsystems.com/shop/cubepro (April 7, 2017)

[8]   Type A Machines, Available: http://www.typeamachines.com/series-1 (April 7, 2017)

[9]   LUMISCAPHE, real-time 3D solutions, http://www.lumiscaphe.com/en/ (April 7, 2016)

FORECAST OF SUSTAINABLE ENERGY DEVELOPMENT IN SLOVENIA

PREDVIDEVANJE RAZVOJA TRAJNOSTNE ENERGETIKE V SLOVENIJI

Matevž Obrecht[ℜ] Matjaž Denac[1]

Keywords: Delphi survey, technology forecasting, sustainable development, energy policy, Slovenia

Abstract

The development of the energy industry is strongly correlated with technology forecasting, which can provide core information for the planning of future energy policy. Energy policy must adhere to the global development paradigm in accordance with energy demand, population growth, global trends, environmental, and legislative restrictions, as well as the specific aspects of specific geographical areas. Reliable data on future trends are crucial for setting up an effective energy policy; therefore, results from a Delphi survey are essential for policy design. This paper presents the most significant findings gathered in the Delphi survey regarding future sustainable energy development in Slovenia. The results have revealed that achieving an increase in energy efficiency and a decrease in final energy consumption is much more important than maintaining low energy prices. The study has also forecast that the prices of all energy sources, including fossil fuels and wood biomass, will increase by 2020 and again by 2030. Delphi also forecast that Slovenia will transition to sustainable energy industry by 2046. The investments favoured by energy experts are small and micro hydro-electric power plants as well as cogeneration units.

ℜ Corresponding author: dr. Matevž Obrecht, University of Maribor, Faculty of Logistics, Department for sustainable logistics and mobility, Mariborska cesta 7, 3000 Celje, Slovenia, Tel.: +386 3 428 5329, E-mail address: matevz.obrecht@um.si,

[1] University of Maribor, Faculty of Economics and Business, Department of technology and entrepreneurial environment protection, Razlagova 14, 2000 Maribor, Slovenia

Povzetek

Razvoj v energetiki je močno odvisen od tehnoloških predvidevanj, ki lahko predstavljajo osnovni vir informacij pri načrtovanju prihodnje energetske politike. Energetska politika se mora navezovati na globalno razvojno paradigmo ob upoštevanju energetskih potreb, demografskih sprememb, globalnih trendov, okoljskih in zakonskih omejitev ter posebnosti posameznih geografskih področij. Za pripravo učinkovite energetske politike potrebujemo zanesljive podatke, ki jih Delphi raziskava z naborom različnih strokovnjakov s področja energetike nedvomno zagotavlja. V prispevku so predstavljene najpomembnejše ugotovitve pridobljene v slovenski Delphi raziskavi o prihodnjem razvoju trajnostne energetske politike v Sloveniji. Rezultati raziskave so pokazali, da je doseganje višje energetske učinkovitosti in zmanjševanje rabe končne energije veliko bolj pomembno od ohranjanja nizkih cen energije. Raziskava je prav tako potrdila predvidevanja, da se bodo cene vseh energentov, vključno s fosilnimi gorivi in lesno biomaso do leta 2020 povečale, še nadaljnje povečevanje cen energentov pa je mogoče pričakovati tudi do leta 2030. Po predvidevanjih Delphi raziskave bo Slovenija prešla v trajnostno energetiko okoli leta 2046. Po mnenju energetskih strokovnjakov so najprimernejše investicije v male- in mikro-hidroelektrarne ter v kogeneracijske enote/v enote za soproizvodnjo toplote in elektrike.

1 INTRODUCTION

While it is true that the future is unpredictable, some future events can be forecast to some extent to prepare for the future (with limitations) and attempt to shape it, *[1]*. In the case of energy policy, the future will be shaped with the goal of minimizing the use of natural resources, particularly conventional energy sources (CES), to raise energy efficiency, to transition to renewable energy sources (RES) and to ensure a secure energy supply.

With technological forecasts, high-quality data on future energy industry development can be obtained that provides a solid foundation for effective and coordinated energy development planning. If forecasts are carried out systematically, professionally and periodically, the shaping of energy policy measures is more effective, can achieve greater positive effects, and be more consistent with the overall development paradigm, *[2]*. Technology foresight, which emerged as a proven instrument of technology policy during the 1950s, has nowadays become one of the essential tools for the creation of technological development throughout the world, *[3]*. In the mid-20th century, people realized that energy and energy sources are scarce. Focusing on technology forecasting in the energy sector the effect of the oil shock in 1973, followed by the first oil crisis in 1979 cannot be ignored. At that time, the Western world, in particular, was faced for the first time with insufficient and insecure oil supplies. The development of the energy industry and energy policy at that time, therefore, demanded the development of new energy models and energy-related technology forecasts in order to foresee the possible future and to prepare energy policies and action measures for it according to a variety of scenarios.

Forecasting future energy development has recently become even more crucial, since the price of energy sources is increasing, constituting a significant share of total costs in the energy industry, *[4]*, as well as in transport and logistics and some other energy-intensive industries. The effective planning of future energy development and forecasting development trends also

enables us to consider the probability and assessment of different scenarios. The IEA, *[5]*, states that future energy development and planning is a core competency for policy decision makers.

One of the tools for such forecasts is the Delphi method which is nowadays widely applied as a valuable future-oriented intuitive foresight tool for the qualitative and quantitative assessment of probable future development, *[3]*, but is rather complicated and very time-consuming.

The intuitive Delphi method is based on trust in the knowledge, expertise and ability of the participating experts to make projections for the future, *[6]*. All identified experts must be extremely well-informed about specific research issues and must have extensive knowledge and information related to relevant energy issues. Because inaccuracies may occur if only one expert makes a forecast, Delphi includes a small number of experts ranging from 10 to 15 top experts on the specific discipline, *[6]*. The number of leading energy experts is severely limited due to the highly specialized research topic. The identification of appropriate and credible experts is crucial, *[1]*, and can be an extremely challenging and time-consuming part of the Delphi survey, *[7, 8]*.

With the Delphi method, we can access and study highly specialized data provided by the participating top experts to form technology forecasts. Delphi methodology has already been widely used for energy-related forecasts such as designing and modelling future energy development in India, *[9]*, to forecasting maritime oil freight flows, *[10]*, or studying future energy industry planning in Spain, *[11]*. Delphi methodology is highly appropriate for predicting future energy sector development; however, it can be used in a range of approaches, as can be seen in a) the study by Makkonen et al., *[12]*, focussing on the effects of different measures for European electricity markets or b) in the study by Hussler et al., *[13]*, focussing on whether diversity of opinions might lead to greater robustness and whether different groups of people (experts vs laypersons) rely on divergent rationalities in composing reliable panels of technological forecasting in the nuclear sector. Wehnert et al., *[14]*, surveyed the energy future of the EU, where researchers performed a) a Delphi survey to analyse the opinions of the involved experts, and b) developed three scenarios with different aspirations for sustainable development. Another study, by Di Zio and Maretti, *[15]*, used the Delphi method to determine the energy sources that are most acceptable or most preferred by the public, political systems and the market. They also studied the weight that these dynamics of acceptability have on global energy movements.

The purpose of this Delphi survey is to forecast detailed future energy development, especially on the Slovenian market with some implications on the EU and the world as well, by 2030 with guidelines and directions for its development by 2050. The aim of the research is to interview relevant Slovenian top energy experts and to integrate their opinion on energy issues to make a technology forecast for different energy-related sectors, to assess the transition time to the sustainable energy industry, to assess the fulfilment of set of renewable energy objectives and sustainability of the Slovenian electricity mix, to forecast energy demand and trends related on energy prices and to set the scale of priority measures for the development of more sustainable energy technology.

2 METHODOLOGY

The Delphi study was conducted in separate content-distributed sections. Due to the large amounts of collected data, this paper only presents the core results of future energy development trends.

The survey was carried out in several stages. First, potential energy experts evaluated as eligible to participate in the study were identified. The selection key included their professional experience; job title, description and field of employment (e.g. government, private company, etc.); education; participation in energy projects and publications in the field of energy in professional and scientific journals. We managed to identify and draw up a credible base of 56 top energy experts in Slovenia from a variety of fields, constituting the core for a Delphi study. These experts were personally contacted, informed about the topic and procedure of the Delphi survey and invited to participate in it. Thirty-four of the contacted experts were willing to cooperate. From the participants, 61% or 20 questionnaires were obtained on time, representing a survey sample.

The Delphi survey was conducted from January 2012 to August 2012. Among the participating experts, 80% of them were men, and 20% were women. The employment period of the experts in the energy sector was above 10 years in 75% of the respondents and more than 15 years in 50% of them, which means that the participating experts are long-time contributors to the energy sector. The structure of cooperating experts is presented in Figure 1.
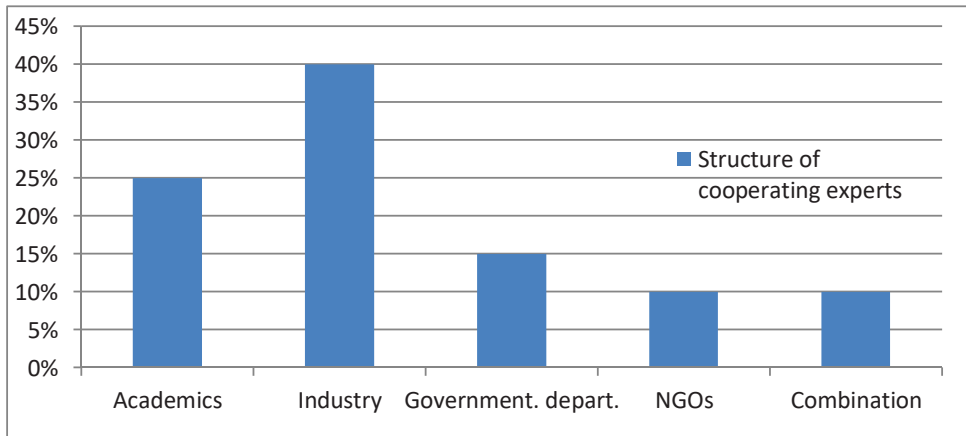

Figure 1: Structure of cooperating top energy experts

Almost two-thirds of the participating experts worked in industry or as academics; others were from governmental departments, NGOs, or a combination of these. Similar classifications of different stakeholders were also in studies by Soner Celiktas and Kocar, *[16]*, Czaplicka-Kolarz et al., *[3]*, and Makkonen et al., *[12]*, etc.

In the Delphi survey, a structured questionnaire was used to examine four lots of energy-related content. The survey was conducted through: "assessment of the importance of sustainable energy development"; "assessment of the accuracy of the study of the factors of sustainable energy development"; "assessment of the accuracy of the developed energy model" and the

most essential part of the research – "a forecast of future sustainable energy development in Slovenia, the EU and the world". Due to the large amounts of obtained data, data analysis was performed in separate lots. This paper presents the essential part of the study for Slovenia – the forecast of future energy development in Slovenia. The remaining parts of the research were or will be published separately.

The acquired quantitative data were analysed using descriptive statistics and a comparative analysis of the various demographic groups of experts (stakeholders). The acquired qualitative data were analysed first with data sampling and then statistically processed.

3   RESULTS AND DISCUSSION

3.1 The outline of the studied results

In this paper, the core results of the Delphi survey are presented in partly separated lots. The first lot (I) presents an assessment of the achievability of the European Union energy-climate objectives, known also as the 20/20/20 objectives targeting to achieve 20 % of renewables in final energy consumption (25% as a specific national target for Slovenia), reducing greenhouse gas (GHG) emissions by 20% and increasing energy efficiency by 20%, all by 2020, as well as an assessment of the impact of the new Slovenian thermal power plant on achieving these legally binding international targets. In the second lot (II), the time frame for the transition from conventional energy to sustainable energy was forecast. Furthermore, in the third lot (III), the direction of energy development was foreseen in accordance with the assessed sustainability of different energy sources in Slovenia. This also studied in a survey about public opinion on energy policy, *[2]*, and results were presented to the participating top energy experts. Differences of the general public (lay-public) and expert judgements are also mentioned and discussed. Furthermore, in the fourth lot (IV), future trends in energy demand in Slovenia were explored and compared with the EU and the world energy demand. These results allow especially Slovenian energy policy decision makers to forecast crucial changes that can be expected in the 21st century.

3.2 Achievability of SLOVENIAN energy policy objectives

The structure of the findings on the achievability of the set objectives in the energy sector is further divided as follows: Experts forecast the probability of achieving the three different goals – the Kyoto protocol (1a), 20/20/20 objectives in general (1b) and a 25% share of renewables in final energy consumption in Slovenia by 2020 (1c).

The participating experts also discussed achieving the Kyoto protocol targets for Slovenia. The crucial issue is that various incompatible and incomplete databases do not allow unequivocally confirming or refuting whether Slovenia will/have fulfilled current Kyoto targets or not. Even during the period of research implementation, differences between the experts on the probability of achieving the Kyoto protocol goals were considerable; however, less than half (41%) believe that targets were achieved (1a). (1b) The experts have also estimated that the chance of achieving the 20/20/20 objectives in Slovenia is 0.387 and (1c) the chance of achieving a 25% share of RES in final energy consumption in Slovenia by 2020 is 0.431.

Since the new block (no. 6) of Šoštanj thermal power plant (TPPŠ) is the largest energy industry project in Slovenia in decades, its impact on achieving the above-mentioned goals (1a, 1b and 1c) was studied as well. The probability of achieving different energy-climate related goals as well as the effects of TPPŠ on the set goals are presented in Table 1.

Table 1: Evaluation of achievement of different international goals relating to the energy industry in Slovenia (n = 20)

Goal	Probability of achieving it (interval from 0 to 1)	Effect of TPPŠ on achieving goals* (interval from -1 to 1)	Probability of achieving it without TPPŠ (interval from 0 to 1)
(1a) Kyoto protocol	0.413	-0.10	0.513
(1b) 20/20/20 objectives	0.387	-0.15	0.537
(1c) 25% of renewables in final energy consumption by 2020 in Slovenia	0.431	-0.05	0.481

* -1 means highly negative impact, and 1 means highly positive impact on achieving the goals

As presented, it will be very difficult to achieve the 20/20/20 objectives in general (probability 0.387); however, the probability of achieving them would be much higher if TPPŠ were not constructed (the probability of achieving these objectives without the reconstruction of TPPŠ would rise to 0.537). Experts have also evaluated that out of all the studied objectives, a 25% share of renewables in final energy consumption in Slovenia by 2020 is the most promising (probability 0.431). RES share at the end of 2014 was 21.9%. (Eurostat, 2016). Due to this high share, the authors evaluate that the probability of Slovenia achieving a 25% share of RES by 2020 is even higher than as assessed by energy experts; however, this share is no longer increasing as fast and as constantly as it was before 2013.

Energy experts have also assessed which target integrated in the 20/20/20 goals is the most difficult to achieve for Slovenia and for the EU in general. Lowering GHG emissions was assessed as the most difficult target to achieve in Slovenia (10 out of 20 experts), followed by achieving increased energy efficiency (EE) (6 out of 20 experts). However, this forecast did not consider reduced feed-in tariffs due to the termination of feed-in tariffs for solar photovoltaics.

On the EU level, in general, the situation is slightly different. For the EU, the most difficult goal to achieve is increasing EE and lowering energy consumption (8 out of 20 experts), followed by increasing the RES share to 20% by 2020 (6 out of 20 experts). Lowering GHG emissions was evaluated as the goal that the EU is most probably going to achieve because only four experts expressed doubt about meeting this target. This is quite realistic, since the EU GHG emissions trend has been declining significantly in recent years, partially due to improved energy efficiency in buildings but partially also due to the economic crisis and the consequently lower level of economic activity between 2009 and 2015, *[17]*.

3.3 Assessment of transition to sustainable energy industry – Slovenia, EU and the world

Furthermore, experts were asked to assess the anticipated time of transition to a sustainably oriented energy industry (lot II). Such an industry was defined in the questionnaire as the end of increasing energy demand, a continually decreasing share of fossil fuels and at least a 30% share of renewables in the national energy mix. Denmark was presented as the best practice case since it has more than halved fossil fuel consumption since 1972, kept the same level of final energy use despite an increase in population and heated areas and plans to have a 30% RES share by 2020.[1] The gathered data were analysed, and the results are presented in Figure 2, separately for Slovenia and compared to the EU and the world. To present the period of this forecast, the Delphi survey implementation time point is also presented.

Figure 2: Evaluated period of forecast transition to sustainably oriented energy industry (Slovenia, EU, and the world)

Average values are presented in Figure 2. Experts beliefs for achieving sustainable energy industry in Slovenia differed significantly, with a group of very optimistic experts (evaluating the period of transition between 2025 and 2030) and one that was less optimistic about it (four experts). On the global level, two of them evaluated that global energy industry will never be sustainably oriented. However, the average grades indicate that Slovenia will transition to a sustainably oriented energy industry in 2045, the EU one year after Slovenia, which makes sense according to current energy statistics and trends and the world approximately 15 years later (in the year 2061). It is clear that the transition to a sustainable energy sector in Slovenia as an EU Member State as well as in the EU in general will be faster than the global transition, since the EU and Slovenia have almost no oil reserves and are, therefore, more interested in independent and locally available energy supply. They are also already significantly investing to achieve this goal, have a common energy policy promoting the use of RES and EE. In another Delphi, survey the results were even more optimistic as Poland's experts forecast that the country will produce at least 30 % of its energy from its local renewables as early as in 2023, *[3]*. This is however debatable, since the share of renewables in Poland's primary energy production is approximately 15%, *[18]*.

---

[1] However, one expert noted that Denmark's relatively sustainable energy situation was extremely expensive and causes high electricity prices

3.4 Sustainability of energy sources and Slovenian energy mix

(III) At this point, the sustainability of different energy sources used in Slovenia was addressed. Sustainability of energy sources was also studied in a survey about public opinion on energy policy [2]. Results presented in Figure 3 show substantial differences in evaluated sustainability of different energy sources. Hydro energy was assessed to be the most sustainable energy source on which Slovenia can rely. The authors believe that this is a realistic evaluation since Slovenia's energy industry is strongly related to hydro-energy and new possibilities for even broader exploitation of hydro energy are being investigated. Public support to hydro energy exploitation is also high, and technical analysis of it shows that it is very appropriate because unlike sun and wind energy that depend on weather conditions, climate, period of the year and are highly volatile, we can predict its availability and manage it to cover peak consumption. Wind and solar energy both got high evaluations in the environmental perspective but rather low in economic appropriateness, mainly due to previously mentioned deficiencies known especially to energy experts but also to the general public.

The second best average grade in all three perspectives on sustainability was assigned to biomass and biogas. Because over 55% of Slovenia is covered by forests, this evaluation also aims that biomass and biogas potential should be exploited to a greater extent and more efficiently in the future of Slovenian energy industry. As expected the lowest environmental grades were assigned to oil and coal, which were also assessed as economically quite appropriate, which was surprising due to controversial issues regarding TPPŠ and economic indicators that reveal TPPŠ is operating negatively already from the beginning and is going to be even more problematic for energy industry economics and sustainability in the future.
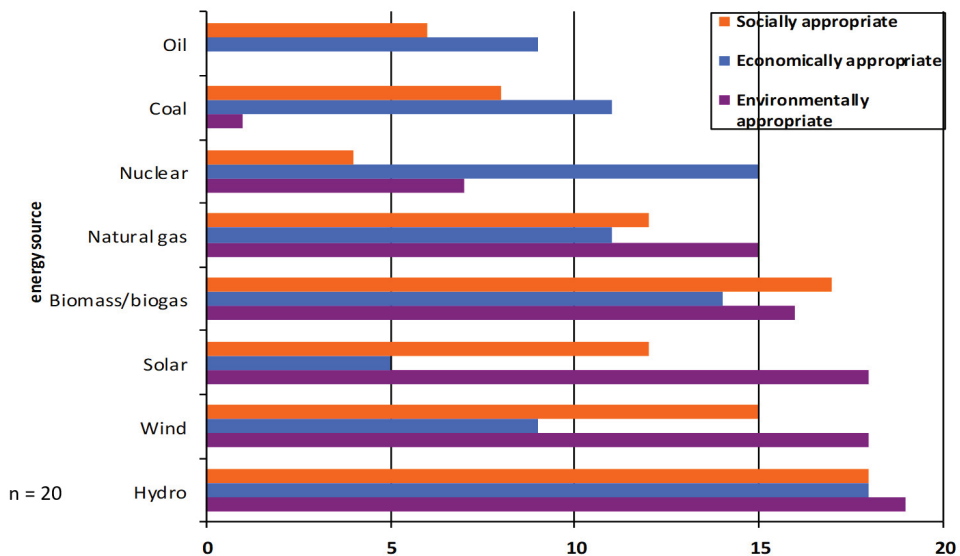

Figure 3: *Appropriateness of different energy sources in Slovenia from social, economic and environmental perspectives*

However, when assessing energy policy priorities, top energy experts and lay public both identified increased energy efficiency, decreased energy use and planning environmentally friendly energy industry as the top energy policy priorities therefore consensus was clear in this case. If we go one step further and consult Hussler's study, *[13]*, in which the variety of judgments within and between experts and lay public was studied, the conclusion was apparently paradoxical: that non-expert judgment is less stable, but not necessarily less accurate, than that of the experts.

3.5   Forecast of energy demand and energy prices for Slovenia

(IV) Since global energy demand has been increasing in recent decades, experts were asked to forecast future energy demand in Slovenia, the EU and the world, along with future prices of different energy sources and electricity, as well as emission allowances. Forecasts were made separately for the time frames until 2020 and from 2020 to 2030.[2] Future energy demand in Slovenia, the EU and the world is further presented in Figure 4.
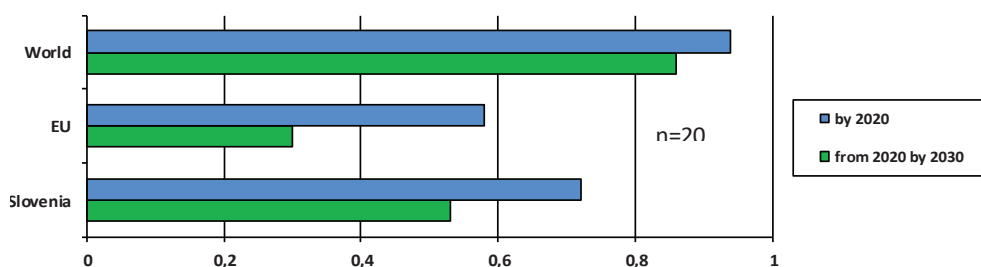

Figure 4: *Forecast of future energy demand in Slovenia, the EU and globally (interval from 0 to 1, where 0 means growth is not possible, and 1 means growth is very possible*

As presented in Figure 4, experts believe that energy demand will increase mostly on the global level by 2020 (95% of all experts believe that global energy demand will rise by 2020) as well as from 2020 to 2030. An increase in energy demand in Slovenia by 2020 will be slightly lower than globally but higher than in the EU and significantly lower from 2020 to 2030. Some experts believe that energy demand in Slovenia will remain constant in the period from 2020 to 2030. The slowest increase is forecast for the EU from 2020 to 2030. A slower increase in energy demand in the EU after 2020 was also projected in other studies, *[17]*. The future economic situation will most probably also have severe impacts on future prices of energy sources and emission allowances, since it is highly dependent on energy demand as the prices of fossil fuels are mainly regulated by OPEC. If Slovenia is able to achieve the transition towards a more sustainable energy industry, energy price volatility could be significantly decreased.

In accordance with energy demand forecasts, energy experts also forecast increasing prices of energy sources and emission allowances in all the studied periods. It was evaluated that fossil

---

[2] In accordance with the time frame of 20/20/20 objectives and their discussed upgrade which is planned to be set by 2030.

fuel prices along with electricity prices will increase most rapidly by 2020. It can be expected that prices will also increase from 2020 to 2030 but less intensively than by 2020. Some energy experts have also forecast the increasing price of wood biomass, *[17]*. However, only the average values are presented in Figure 4. A more detailed data analysis has shown that these assumptions differ significantly from each other, since some experts have forecast strong growth and others a decrease in wood biomass prices. The wood biomass price is probably more difficult to forecast since studies dealing with future biomass prices are rare. However, Slovenia suffered severe freezing rain in February 2014 which damaged 42% (3.5 million cubic meters) of Slovenian woods, an amount equal to the annual timber removal. The trend of increasing prices of wooden biomass, seen from 2009, consequently changed and prices (especially wooden biomass for heating and energy use) were in 2014 much lower because the wooden biomass supply has rapidly increased, *[19]*. In addition, further wind breakage destroyed additional 1 million cubic meters of wood in 2016 and 2017.

4   CONCLUSION AND POSSIBLE IMPLICATIONS

The Delphi method proved to be a successful research method in studying the future technology development of a specific sector. It was conducted to shed light on an issue that is highly topical in Slovenia, the EU and the world: the forecast of future technological development of the energy sector and its influence on the transition to a sustainable energy industry.

The Delphi method revealed critical issues relating to the probability of achieving the 20/20/20 goals especially due to the negative effect of TPPŠ on Slovenian national energy statistics, increasing future energy demand by 2030, and the forecast increase in oil prices (despite the significant decrease in oil prices at the beginning of 2015), natural gas prices, wooden biomass prices, as well as emission allowance prices. The study revealed that experts believe that future energy policy must be radically transformed since top energy policy priorities were 1) the reduction of energy use, 2) an increase in EE, and 3) development of an environmentally friendly energy industry.

Since leading energy experts have forecast that the EU and Slovenia as a member state will transition to a sustainable energy industry by 2046, the top priorities will most likely be realized, at least to some extent. This is especially important for the EU and its Member States, such as Slovenia, since there are no significant oil reserves, but the energy sector is already heavily dependent on imported oil. As this dependency can lead to economic and socio-political risk, energy policies based on prudent and efficient energy use and energy production from local renewables are crucial for the long-term socio-political stability of the EU as well as rising standards of living on the local level.

References

[1]   **K. Cuhls:** *From forecasting to foresight processes – new participative foresight activities in Germany*, Journal of Forecasting. vol. 22, Iss. 2-3, p.p. 93-111, 2003

[2]   **M. Obrecht:** *Study of factors for sustainable energy development modelling. Doctoral dissertation*, Maribor, Faculty of Economics and Business, 2013

[3]   **K. Czaplicka-Kolarz, K. Stanczyk and K. Kapusta:** *Technology foresight for a vision of energy sector development in Poland till 2030. Delphi survey as an element of technology foresighting.* Technological Forecasting and Social Change. vol. 76, iss. 3, p.p. 327-338, 2009

[4]   **M. Obrecht and M. Denac:** *A study of key factors for energy policy modelling.* Naše gospodarstvo, vol. 58, iss. 3-4, p.p. 28-37, 2012

[5]   **IEA**: *Energy Technology Perspectives 2016 – Towards Sustainable Urban Energy Systems*, Paris, IEA, 2016

[6]   **B. Pregrad and V. Musil:** *Technological systems and integrated environmental protection,* Textbook, Maribor, Faculty of Economics and Business, 2001 (in Slovenian language)

[7]   **H. Grupp and H. Linstone:** *National technology foresight around the globe, resurrection and new paradigms*. Technological Forecasting and Social Change, vol. 60, p.p. 85–94, 1999

[8]   **M. Obrecht and M. Denac:** *A sustainable energy policy for Slovenia: considering the potential of renewables and investment costs.* Journal of renewable and sustainable energy, vol. 5, iss. 3, 2013

[9]   **S. Iniyan and K. Sumathy:** The application of a Delphi technique in the linear programming optimization of future renewable energy options for India. *Biomass and Bioenergy,* vol. 24, p.p. 39-50, 2003

[10] **J. Dinwoodie, S. Tuck and P. Rigot-Müller:** *Maritime oil freight flows to 2050: Delphi perceptions of maritime specialists*. Energy Policy. vol. 63, p.p. 553-561, 2013

[11] **Terrados, J., Almonacid, G. and Pérez-Higueras, P.** 2009. *Proposal for a combined methodology for renewable energy planning. Application to a Spanish region.* Renewable and Sustainable Energy Reviews, vol. 13, iss. 8, p.p. 2022-2030, 2009

[12] **M. Makkonen, S. Pätäri, A. Jantunen and S. Viljainen:** *Competition in the European electricity markets – outcomes of a Delphi study*, Energy Policy, vol. 44, p.p. 431-440, 2012

[13] **C. Hussler, P. Muller and P. Rondé:** *Is diversity in Delphi panelist groups useful? Evidence from a French forecasting exercise on the future of nuclear energy.* Technological Forecasting and Social Change, vol. 78, iss. 9, p.p. 1642-1653, 2011.

[14] **T. Wehnert, J.P. López Araguás, O. Bernardini, L. Jaworski, B. Holst Jørgensen, W. Jörß, O. Nielsen, A. Ninni, A. Oniszk-Poplawska and D. Velte:** *European energy futures 2030*, Berlin Heidelberg, Springer-Verlag, 2007

[15]   **S. Di Zio and M. Maretti:** *Acceptability of energy sources using an integration of the Delphi method and the analytic hierarchy process.* Quality and Quantity. Published online in September 2013

[16]   **M. Soner Celiktas and G. Kocar:** From potential forecast to foresight of Turkey's renewable energy with Delphi approach, *Energy,* vol. 35, iss. 5, p.p. 1973-1980, 2010

[17]   **M. Obrecht and M. Denac:** *Technology forecast of sustainable energy development prospects*, Futures, vol. 84 part A, p.p. 12-22, 2016

[18]   **Eurostat**: *Energy statistics – quantities.* [online]. Available on: http://epp.eurostat.ec.europa.eu/portal/page/portal/energy/data/main_tables (15.11.2017), 2016

[19]   **J. Bavčar:** *The worst icerain in Slovenia.* Delo in dom. [online]. Available on: http://www.deloindom.si/sadovnjaki/najhujsi-zledolom-v-sloveniji   (11.1.2016), 2014 (in Slovenian language)

MAIN TITLE OF THE PAPER
SLOVENIAN TITLE

Author[1], Author [2], Corresponding author[ℜ]

Keywords: (Up to 10 keywords)

Abstract

Abstract should be up to 500 words long, with no pictures, photos, equations, tables, only text.

Povzetek

(Abstract in Slovenian language)

Submission of Manuscripts: All manuscripts must be submitted in English by e-mail to the editorial office at jet@um.si to ensure fast processing. Instructions for authors are also available online at http://www.fe.um.si/en/jet/author-instructions.html.

Preparation of manuscripts: Manuscripts must be typed in English in prescribed journal form (MS Word editor). A MS Word template is available at the Journal Home page.

A title page consists of the main title in the English and Slovenian language; the author(s) name(s) as well as the address, affiliation, E-mail address, telephone and fax numbers of author(s). Corresponding author must be indicated.

Main title: should be centred and written with capital letters (ARIAL bold 18 pt), in first paragraph in English language, in second paragraph in Slovenian language.

Key words: A list of 3 up to 6 key words is essential for indexing purposes. (CALIBRI 10pt)

Abstract: Abstract should be up to 500 words long, with no pictures, photos, equations, tables, - text only.

Povzetek: - Abstract in Slovenian language.

Main text should be structured logically in chapters, sections and sub-sections. Type of letters is Calibri, 10pt, full justified.

ℜ Corresponding author: Title, Name and Surname, Organisation, Department, Address, Tel.: +XXX x xxx xxx, E-mail address: x.x@xxx.xx

[1] Organisation, Department, Address

[2] Organisation, Department, Address

<u>Units and abbreviations</u>: Required are SI units. Abbreviations must be given in text when first mentioned.

<u>Proofreading</u>: The proof will be send by e-mail to the corresponding author in MS Word's Track changes function. Corresponding author is required to make their proof corrections with accepting or rejecting the tracked changes in document and answer all open comments of proof reader. The corresponding author is responsible to introduce corrections of data in the paper. The Editors are not responsible for damage or loss of submitted text. Contributors are advised to keep copies of their texts, illustrations and all other materials.

The statements, opinions and data contained in this publication are solely those of the individual authors and not of the publisher and the Editors. Neither the publisher nor the Editors can accept any legal responsibility for errors that could appear during the process.

<u>Chapter examples:</u>

1   MAIN CHAPTER

(Arial bold, 12pt, after paragraph 6pt space)

1.1   Section
(Arial bold, 11pt, after paragraph 6pt space)

1.1.1 Sub-section

(Arial bold, 10pt, after paragraph 6pt space)

Example of Equation (lined 2 cm from left margin, equation number in normal brackets (section. equation number), lined right margin, paragraph space 6pt before in after line):

$$\text{Equation} \tag{1.1}$$

Tables should have a legend that includes the title of the table at the top of the table. Each table should be cited in the text.

Table legend example:

Table 1: *Name of the table (centred, on top of the table)*

Figures and images should be labelled sequentially numbered (Arabic numbers) and cited in the text – Fig.1 or Figure 1. The legend should be below the image, picture, photo or drawing.

Figure legend example:

Figure 1: Name of the figure (centred, on bottom of figure, photo, or drawing)

References

[1]   **N. Surname:** *Title,* Journal Title, Vol., Iss., p.p., Year of Publication

[2]   **N. Surname:** *Title,* Publisher, Year of Publication

[3]   **N. Surname:** *Title* [online], Publisher or Journal Title, Vol., Iss., p.p., Year of Publication. Available: website (date accessed)

Examples:

[1]   **J. Usenik**: *Mathematical model of the power supply system control*, Journal of Energy Technology, Vol. 2, Iss. 3, p.p. 29 – 46, 2009

[2]   **J. J. DiStefano, A.R. Stubberud, I. J. Williams**: *Theory and Problems of Feedback and Control Systems*, McGraw-Hill Book Company, 1987

[3]   **T. Žagar, L. Kegel:** *Preparation of National programme for SF and RW management taking into account the possible future evolution of ERDO* [online], Journal of Energy Technology, Vol. 9, Iss. 1, p.p. 39 – 50, 2016. Available: http://www.fe.um.si/images/jet /Volume 9_Issue1/03-JET_marec_2016-PREPARATION_OF_NATIONAL.pdf (7. 10. 2016)

Example of reference-1 citation: In text *[1],* text continue.

Nomenclature

(Symbols)	(Symbol meaning)
t	time